Front. Earth Sci. 2024, 18(1): 148–171
https://doi.org/10.1007/s11707-022-1071-5

RESEARCH ARTICLE

Constraints of palaeoenvironment on organic matter of Benxi Formation shale and discussion on enrichment mechanism under different facies

Qianyang HE[1,2,3], Delu LI (✉)[1,2,3], Qiang SUN[1,2,3], Jianwen GAO[4], Haibin LI[1,2,3], Xinhu LI[1,2,3], Xiaochen ZHAO[1,2,3], Shaofei WANG[5], Gaozhe JI[1,2,3]

1 College of Geology and Environment, Xi'an University of Science and Technology, Xi'an 710054, China
2 Shaanxi Provincial Key Laboratory of Geological Support for Coal Green Exploitation, Xi'an University of Science and Technology, Xi'an 710054, China
3 Geological Research Institute for Coal Green Mining, Xi'an University of Science and Technology, Xi'an 710054, China
4 Research Institute of Exploration and Development, PetroChina Changqing Oilfield Company, Xi'an 710018, China
5 School of Civil Engineering and Architecture, Shaanxi University of Technology, Hanzhong 723001, China

Abstract As a hydrocarbon-rich sedimentary basin in China, the Ordos Basin has enormous potential for shale gas resources. The shale of the Upper Carboniferous Benxi Formation is rich in organic matter, however, its palaeoenvironment and organic matter enrichment mode are yet to be revealed. In this study, the geochemical characteristics of the shale of the Benxi Formation in the east-central part of the Ordos Basin were analyzed to investigate its palaeoenvironment. At the same time, the organic matter enrichment modes in different sedimentary facies were compared and analyzed. The results indicate that: 1) the shale of the Benxi Formation was mainly deposited on the continental margin and strong terrestrial clastic input; 2) the deposition period of the Benxi Formation shale had a hot and humid climate with high palaeoproductivity and local volcanic hydrothermal fluid, and a high sedimentation rate with the strong stagnant environment. The bottom water was in dysoxic conditions and a semi-saline deposition environment; 3) multiple factors, such as palaeoproductivity, volcanic hydrothermal, redox conditions, and palaeosalinity interact to influence the enrichment of shale organic matter in Benxi Formation; 4) the organic matter enrichment modes of continental, marine-continental transitional, and marine shales can be classified into three types: "production mode", "hybrid mode of preservation and production", and "preservation mode", respectively. This study provides a reference for the organic matter enrichment mode, shale gas formation conditions, and core area evaluation in these marine-continental transitional shales, and also offers new guidance for exploration ideas for shale gas in different sedimentary facies.

Keywords Benxi Formation, shale, palaeoenvironment, organic matter enrichment, facies

Received November 1, 2022; accepted April 10, 2023

E-mail: lidelu322@126.com

1 Introduction

Shale gas is a crucial hydrocarbon resource, which is distributed worldwide and has enormous potential for development (Rimmer et al., 2004; Ding et al., 2013; Tang et al., 2014; Khaled et al., 2022). Chinese shale is characterized by its wide distribution, high organic matter content, and large resources. According to their depositional environment, they can be classified into three kinds of types: continental, marine-continental transitional, and marine shales, among which marine-continental transitional shale accounts for a higher proportion and has better development prospects (Wei et al., 2020; Zhang et al., 2021). The Carboniferous to Permian was a vital period in the transformation of the depositional environment of China into a marine-continental transitional facies. Transitional shale is widely deposited in the Ordos, Tarim, and Junggar Basins and other regions. The marine-continental transitional shale in the Ordos Basin is developed in the Benxi Formation, Taiyuan Formation, and Shanxi Formation (Song et al., 2016; Yang et al., 2019). The Benxi Formation, as a typical organic-rich shale of the marine-continental transitional facies, has enormous potential for development.

Over the last few decades, the geochemical characteristics, depositional environments, organic matter enrichment modes, deposition modes, and gas-in-place content of organic matter-rich shale have been extensively studied (Li et al., 2019a; Chen et al., 2020; Li et al., 2021; Yu et al., 2022). In general, organic matter enrichment modes can be divided into two types. The "production mode" emphasizes the influence of factors such as palaeoclimate, palaeoproductivity, and terrestrial clastic input on organic matter enrichment, while the "preservation mode" emphasizes the control of organic matter by factors such as redox conditions, palaeosalinity, and sedimentation rate (Ma et al., 2019; Awan et al., 2020; Khaled et al., 2022; Wu et al., 2022a; Zhou et al., 2022). In terms of the enrichment of shale organic matter by palaeosalinity, it has been widely concluded that with the increase of palaeosalinity, organic matter increases first and then decreases. Shale developed in semi-saline-alkaline environment is the most ideal target for exploration and development. (He et al., 2018; Hu et al., 2018). Commonly, geochemical parameters are used to reconstruct the palaeoenvironment, while CIA, Sr/Cu, and C_{value} can be widely used in evaluating palaeoclimatic conditions quantificationally. P/Ti and Mo are used as geochemical indicators of palaeoproductivity, and Fe/Ti and (Fe + Mn)/Ti are used to restore volcanic hydrothermal fluid (Nesbitt and Young, 1982; Yamamoto, 1987; Bernárdez et al., 2008; Stock et al., 2017; Ma et al., 2019; Wang et al., 2020). As a result of previous studies, Aluminum (Al), Titanium (Ti), and Thorium (Th), which are transported into the water column and are less susceptible to diagenesis and weathering, can often indicate the input of terrestrial clastic, while $(La/Yb)_N$ can be used to evaluate the rate of sedimentation (Tyson, 2001; Ding et al., 2015; Doner et al., 2019). Rare earth and trace elements vary in enrichment intensity under different redox conditions, and trends in the ratios of Ni/Co, U/Th, and V/(V + Ni) are commonly used to characterize changes in the redox environment of the deposition site. Palaeosalinity is usually used to identify the extent and duration of water intrusion, while the ratios of Sr/Ba and Th/U, which are composed of trace elements sensitive to water column salinity, are common indicators of palaeosalinity (Jones and Manning, 1994; Wignall and Twitchett, 1996; Stüben et al., 2002; Rimmer, 2004; Zhang et al., 2008; Jenkyns et al., 2017). The organic matter enrichment modes of marine and continental shales have been extensively studied. The continental shale is mainly developed in lake basins, where the paleoclimate was cold and dry or warm and humid during the deposition period, and the water reducibility and palaeosalinity were low. Organic matter enrichment is mainly influenced by redox conditions and palaeoproductivity, with palaeoproductivity being the main controlling factor (Yu et al., 2022). Marine shale is mainly deposited on continental margins, where the climate is warm and wet and the water column is dominated by reducing conditions and high palaeosalinity. There is also possible submarine hydrothermal influences, where organic matter enrichment is influenced by multi-factor and is usually dominated by a preservation model (Zhang et al., 2018a; Li et al., 2019a; Li et al., 2020). The transitional sedimentary environment is rich in shale, but its organic matter enrichment pattern is lacking, mainly concentrated in the Shanxi–Taiyuan Formation in the Ordos Basin, the Longtan Formation in the Sichuan Basin, and the Cuizhuang Formation in the Yuncheng Basin (Liu et al., 2018; Li et al., 2019c; Chen et al., 2020; Wei et al., 2020; Khaled et al., 2022; Yang et al., 2022). In terms of gas-in-place content in shales, previous work has developed a gas-in-place content calculation model based on a carbon isotope fractionation model and evaluated gas-adsorbed ratio, providing a powerful tool for evaluating key parameters of unconventional gas resources (Li et al., 2022). The above studies have systematically investigated the enrichment mode of organic matter shales, but the geochemical characteristics of the marine-continental transitional shale of the Benxi Formation remain to be clarified. Their palaeoenvironmental conditions and the mechanisms influencing organic matter enrichment are yet to be revealed, while the comparison of the differences in organic matter enrichment mechanisms between different sedimentary facies is open to debate.

This research systematically sampled shales of the Upper Carboniferous Benxi Formation in the east-central part of the Ordos Basin. Organic geochemical tests and elemental geochemical analyses were conducted to recover the palaeoenvironment of the stratigraphic deposition period in this area, explore the influences on the palaeo-depositional environment that affected organic matter enrichment (for instance, palaeoclimate, water redox conditions, palaeosalinity, palaeoproductivity, volcanic hydrothermal fluid, and sedimentation rate), and the enrichment mechanism of organic matter was revealed. The differences in organic matter enrichment mechanisms of shales under different sedimentary facies are also compared and analyzed. These results provide a reference for shale gas exploration and reservoir selection.

2 Geological setting

The Early Palaeozoic Middle Ordovician Ordos Basin was in the stage of marginal rifting and intra-land depression, and the main body of the basin is a marine sedimentary environment with carbonate rocks deposited on metamorphic rocks at the base of the basin during the

Taurus and Metamorphic periods. In the Early-Late Palaeozoic, the basin entered a stage of circumferential collisional orogeny, and the Ordos basin was uplifted and subjected to long-term exfoliation. In the end of Late Paleozoic, circumferential rifting occurred and the basin receded, and the sedimentary background was a marine and land interactive sedimentary system, when the North China Plate on which the Ordos Basin is located was in the northern hemisphere, closer to the equator (Fig. 1(a)). The Mesozoic basin underwent intra-land depression. The basin margins were uplifted and lifted off as a whole and it had a terrestrial sedimentary environment. The Cenozoic basin perimeter was gradually fractured to form the present-day tectonic pattern (Yang et al., 2005; Ding et al., 2013; Li et al., 2019b). The basin consists of six primary tectonic units: the Yimeng uplift, the Weibei uplift, the Tianhuan sag, the Yishaan slope, the Jinxi folding belt, and the western edge thrust belt (Tang et al., 2014). The Ordos Basin underwent transformation through marine to marine-continental transitional to

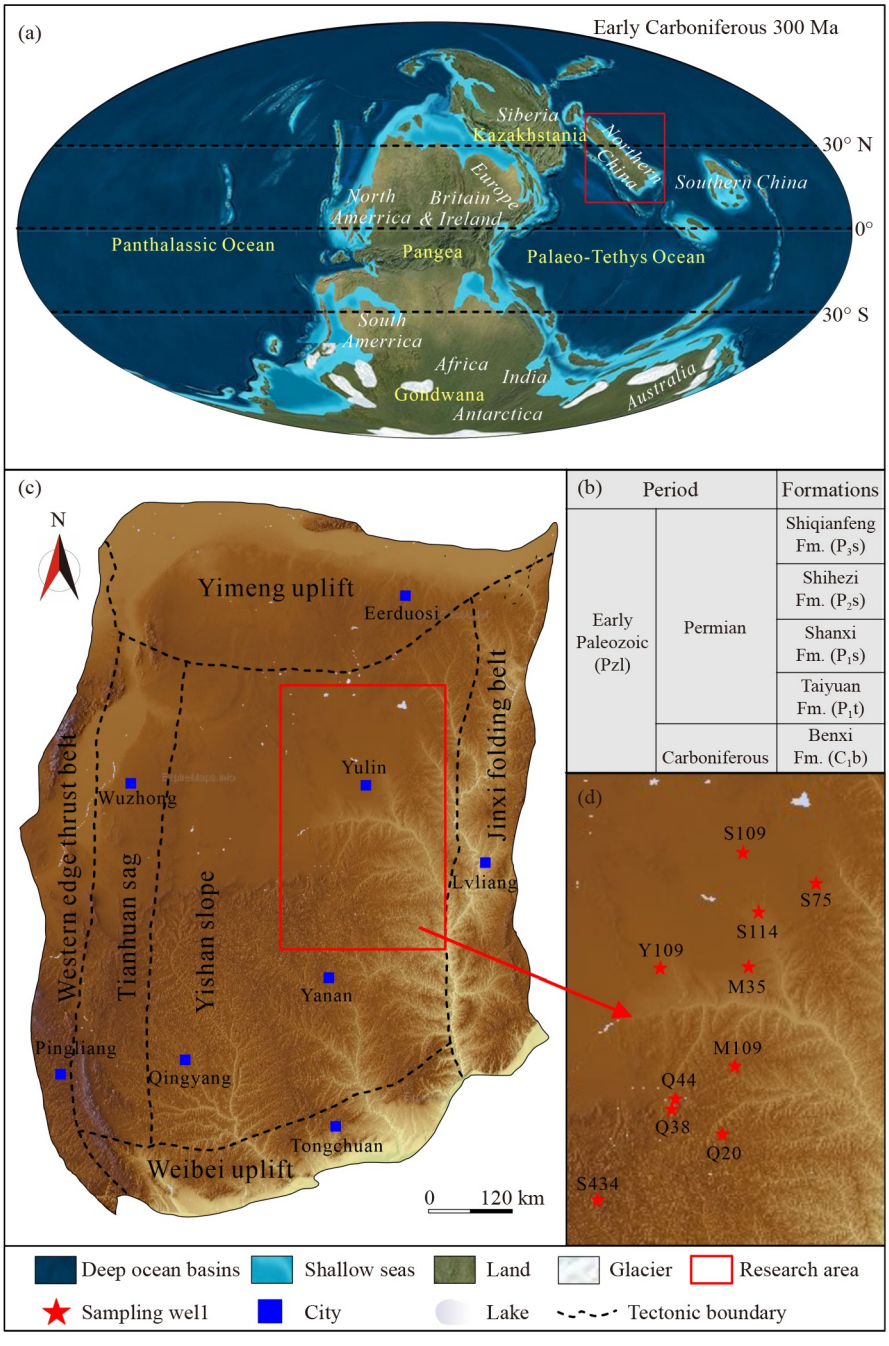

Fig. 1 (a) Late Carboniferous (about 300 Ma) global paleography (base map is from Deeptimemaps website). (b) Distribution map of Early Paleozoic. (c) Tectonic location map. (d) Sampling well location map in Ordos Basin (modified from Dong et al., 2020).

continental-phase sedimentary environments during the Palaeozoic. The Carboniferous-Permian stratigraphy of the marine-continental transitional facies has developed, from bottom to top, in five Formations: Benxi, Taiyuan, Shanxi, Shihezi, and Shiqianfeng, among which the Benxi Formation is the marine-continental transitional facies with deltaic and barrier coastal sedimentation, and the research area is situated at the middle-eastern part of the Yishaan slope, mainly developing gray and gray-brown shales and light gray sandstones (Figs. 1(b)−1(d)) (Peters and Cassa, 1994; Li et al., 2019b; Guo, 2020).

3 Sample preparation and testing

3.1 Sample preparation

The 16 shale core samples in this study were obtained from 10 wells including M35, M109, and Q20 of the Benxi Formation in the central-eastern part of the Ordos Basin (Fig. 1(d)). The rock samples were dried after several washes with deionised water in an ultrasonic environment, then ground to 200 mesh in an agate mortar and subjected to geochemical testing and analysis, including total organic carbon (TOC) and major and trace element tests.

3.2 Test procedure

TOC was tested using a Vario TOC Total Organic Carbon analyzer from Element, Germany, using the infrared absorption method. A 200 mesh powdered sample of 20mg was weighed and subjected to a stream of oxygen at 950°C to oxidise the solid carbon to carbon dioxide. The resulting gas is tested through a carbon dioxide infrared detection cell and converted to the relative content of organic carbon. The test method is performed according to GB/T 19145-2003.

The experimental procedure of the main element tests was referenced from GB/T 14506.28-2010 (Yang et al., 2020). The 200 mesh powdered shale samples were placed in an open muffle furnace at 950°C and dissolved in a mixture of $HClO_4$ and HF. X-ray fluorescence (XRF) measurements were carried out using a combination of AA-6800 atomic absorption spectroscopy and UV-2600 UV-Vis spectrophotometer.

For trace and rare earth elements, 200 mesh powdered samples were dissolved in a mixture of HNO_3, HF, and $HClO_4$ in a microwave oven and extracted with aqua regia after 5 h of digestion at 230°C to make a final 50 mL solution. The prepared liquid sample was measured by a Perkin Elmer SciexElan 6000 inductively coupled plasma mass spectrometer (ICP-MS). The test accuracy was strictly controlled and the analytical uncertainty was kept within 1% (the test procedure was following GB/T 14506.30-2010 standard).

4 Results

4.1 Organic matter abundance

The TOC content of shale samples in the study area ranges from 0.79 wt% to 9.83 wt%, the mean value was 3.37 wt% (Table 1). The mean TOC content of the shale samples was higher than 2 wt%, and a TOC between 2 wt% and 4 wt% is considered a good hydrocarbon source rock abundance criterion based on the previously proposed criteria for evaluating organic matter abundance in hydrocarbon source rocks (Peters and Cassa, 1994). Therefore, the Benxi Formation shale has excellent hydrocarbon source rock potential.

4.2 Main element characteristics

The main elements of the shale of the Benxi Formation are SiO_2 as the main component, with a content of 51.36−92.30 wt% (average 61.75 wt%), then Al_2O_3, Fe_2O_3, and K_2O with average contents of 27.64 wt%, 6.30 wt%, and 1.90 wt%, respectively. The remaining main element concentrations are less than 1 wt% (Table 2). Relative to the Upper Continental Crust (UCC) mean counterparts, the Na_2O, MgO, P_2O_5, K_2O, CaO, and MnO contents of the Benxi Formation shale show significant deficits, while Al_2O_3, TiO_2, and Fe_2O_3 are relatively enriched (Fig. 2(a)).

4.3 Trace element characteristics

Trace elements in sedimentary rocks are often used to

Table 1 The TOC content of the shale samples

Well	Sample ID	Sampling depth/m	TOC/wt%
M35	BX01	2376.38	2.25
M109	BX02	2377.86	2.83
M109	BX03	2379	4.97
M109	BX04	2379.36	5.5
M109	BX05	2405.17	1.99
Q20	BX06	2760.46	2.45
Q38	BX07	2879.56	1.32
Q44	BX08	3020.1	9.83
Q44	BX09	3022.46	1.94
S434	BX10	3530.25	2.32
S75	BX11	2150.81	5.02
S114	BX12	2338.88	3.08
S114	BX13	2348.76	4.04
S109	BX14	2386.23	0.79
Y109	BX15	2548.48	1.1
Y109	BX16	2551.29	4.52
Avg.		2590.94	3.37

Table 2 Main element characteristics of shale samples (wt%)

Sample ID	Na_2O	MgO	Al_2O_3	SiO_2	P_2O_5	K_2O	CaO	TiO_2	MnO	Fe_2O_3
BX01	0.41	0.55	27.72	61.58	0.057	1.84	0.41	0.60	0.030	6.81
BX02	0.47	0.55	30.36	65.31	0.017	1.64	0.18	0.58	0.003	0.89
BX03	0.43	0.49	27.71	67.36	0.019	1.20	0.25	0.55	0.006	1.98
BX04	0.41	0.53	26.17	63.79	0.018	1.26	0.26	0.51	0.014	7.05
BX05	0.60	0.78	39.76	51.36	0.031	3.60	0.35	0.94	0.011	2.57
BX06	0.56	1.05	25.92	61.85	0.105	4.17	0.65	0.62	0.027	5.05
BX07	0.28	0.33	20.62	66.43	0.027	1.01	0.93	0.71	0.021	9.66
BX08	0.09	0.67	2.97	92.30	0.127	0.49	0.21	0.07	0.480	2.81
BX09	0.38	0.98	38.17	46.57	0.144	1.18	1.01	0.90	0.108	10.55
BX10	0.25	1.07	20.74	65.69	0.080	2.24	0.54	0.73	0.079	8.60
BX11	0.35	0.23	30.26	58.30	0.021	0.80	0.26	0.85	0.008	8.92
BX12	0.46	0.35	42.82	52.08	0.044	1.26	0.27	1.02	0.009	1.69
BX13	0.17	0.54	14.55	59.23	0.483	1.75	2.23	0.31	0.152	20.58
BX14	0.38	0.38	38.65	51.58	0.018	1.24	0.50	1.22	0.012	6.01
BX15	0.75	1.01	26.09	57.91	0.116	5.62	0.97	0.83	0.023	6.68
BX16	0.35	0.27	29.73	66.73	0.007	1.03	0.15	0.85	0.012	0.88
Avg.	0.40	0.61	27.64	61.75	0.082	1.90	0.57	0.71	0.062	6.30
UCC	3.27	2.48	15.40	66.00	0.150	2.80	3.59	0.64	0.100	5.04

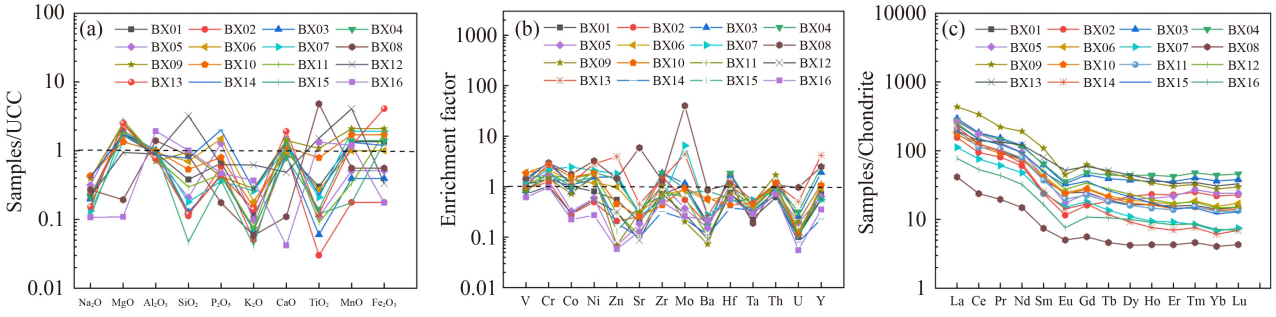

Fig. 2 UCC normalized distribution maps for (a) main elements and (b) trace elements. (c) Standardised map of chondrites for rare earth elements.

reconstruct their palaeoenvironment during the time of deposition. This study mainly considered 14 trace elements, For instance, V, Cr, and Co (Table 3). The elemental enrichment factor (EF) is used to quantitatively describe the enrichment or deficit of trace elements in shales. It is calculated as EF = $(X_{sample}/Al_{sample})/(X_{UCC}/Al_{UCC})$ (Wedepohl and Earth, 1971; McLennan, 2001). Compared to UCC standards, the Benxi Formation shale is relatively enriched in V, Cr, Co, Ni, Mo, U, and Y (EF > 1), while Zn, Sr, Zr, Ba, Hf, Ta, Th, and U are deficient (EF < 1; Table 4).

4.4 Rare earth element characteristics

The rare earth elements (REE) results for Benxi Formation Shale and corresponding standard values, such as Chondrite, are shown in Table 5 (Taylor and McLennan, 1995). Total rare earth elements (ΣREE) variability in the Benxi Formation shale ranges from 50.48 to 621.49 ppm (mean 274.23 ppm), significantly greater than that of the North American Shale Complex (NASC; 173.21 ppm; Haskin et al., 1968) and the Upper Continental Crust (UCC; 146.37 ppm; McLennan, 2001), a little more than the Post-Archean Australian Shale (PAAS; 204.12 ppm; Taylor and McLennan, 1985)). The light rare earth elements (ΣLREE) and heavy rare earth elements (ΣHREE) averaged 247.66 ppm and 26.56 ppm, respectively, and the ratio of light rare earth elements / heavy rare earth elements (ΣLREE/ΣHREE) ranges from 5.63 to 19.52 (average 10.04; Table 5), which is higher than those of North American Shale (7.50), indicating that the LREEs in the shale of Benxi Formation is more enriched than the HREEs. The values of $(La/Yb)_n$, $(La/Sm)_n$, and $(Gd/Yb)_n$ can be used to indicate the

Table 3 Trace element characteristics in shale samples (ppm)

Sample ID	V	Cr	Co	Ni	Zn	Sr	Zr	Mo	Ba	Hf	Ta	Th	U	Y
BX01	119.04	90.32	17.89	28.96	69.68	126.07	243.39	2.82	190.52	7.87	0.93	11.77	3.97	29.29
BX02	107.04	85.67	5.63	19.47	29.13	176.40	590.93	1.61	186.73	19.54	1.61	20.96	4.93	44.69
BX03	89.18	118.90	13.98	55.25	199.78	188.35	630.50	3.13	158.15	17.27	1.46	21.65	10.08	75.59
BX04	80.82	114.71	16.98	66.96	165.59	181.07	596.72	2.32	156.69	18.22	1.35	21.55	11.77	91.35
BX05	214.40	161.03	8.45	30.45	12.28	164.23	533.79	1.45	214.23	16.68	1.76	23.49	11.00	35.99
BX06	192.11	125.06	22.35	40.11	118.37	182.60	220.41	2.13	495.46	6.51	1.52	18.31	4.76	34.68
BX07	94.25	103.54	32.70	55.69	172.36	123.53	135.94	13.11	205.58	4.16	1.61	11.50	3.21	16.22
BX08	16.72	20.00	3.41	12.47	20.00	397.03	47.84	11.55	90.12	1.27	0.08	2.22	4.09	10.48
BX09	131.32	127.62	17.81	85.20	12.22	266.78	484.93	0.75	99.31	15.15	2.60	44.85	11.19	61.03
BX10	149.71	129.75	20.99	49.34	43.54	122.43	110.76	1.91	426.26	3.38	1.37	17.12	3.39	30.76
BX11	132.79	117.31	28.34	69.81	42.75	74.77	304.98	1.80	108.31	8.94	2.01	22.09	6.24	24.16
BX12	119.20	98.46	8.30	30.64	61.27	83.69	380.82	1.20	139.88	11.64	1.77	21.33	6.82	34.58
BX13	58.49	91.14	11.11	53.54	263.98	148.73	259.24	6.23	139.65	7.05	1.07	11.47	10.53	86.74
BX14	196.54	271.52	27.20	70.46	33.45	87.58	152.60	0.86	152.72	5.50	1.88	17.96	4.40	12.64
BX15	173.81	84.87	21.65	50.74	15.79	239.35	206.60	1.92	763.54	5.65	1.26	14.60	3.93	33.64
BX16	71.22	65.37	4.32	10.48	7.97	87.59	181.60	0.75	225.92	6.61	1.22	14.56	2.36	14.93
Avg.	121.66	112.83	16.32	45.60	79.26	159.88	317.57	3.35	234.57	9.71	1.47	18.46	6.42	39.80
UCC	60.00	35.00	10.00	20.00	71.00	350.00	190.00	1.50	550.00	5.80	2.20	10.70	2.80	22.00

Table 4 Enrichment factors for trace elements in shale samples

Sample ID	EF(V)	EF(Cr)	EF(Co)	EF(Ni)	EF(Zn)	EF(Sr)	EF(Zr)	EF(Mo)	EF(Ba)	EF(Hf)	EF(Ta)	EF(Th)	EF(U)	EF(Y)
BX01	1.10	1.43	0.99	0.80	0.55	0.20	0.71	1.05	0.19	0.75	0.24	0.61	0.10	0.74
BX02	0.90	1.24	0.29	0.49	0.21	0.26	1.58	0.54	0.17	1.71	0.37	0.99	0.11	1.03
BX03	0.83	1.89	0.78	1.54	1.56	0.30	1.84	1.16	0.16	1.66	0.37	1.12	0.25	1.91
BX04	0.79	1.93	1.00	1.97	1.37	0.30	1.85	0.91	0.17	1.85	0.36	1.19	0.31	2.44
BX05	1.38	1.78	0.33	0.59	0.07	0.18	1.09	0.37	0.15	1.11	0.31	0.85	0.19	0.63
BX06	1.90	2.12	1.33	1.19	0.99	0.31	0.69	0.84	0.54	0.67	0.41	1.02	0.13	0.94
BX07	1.17	2.21	2.44	2.08	1.81	0.26	0.53	6.53	0.28	0.54	0.55	0.80	0.11	0.55
BX08	1.45	2.96	1.77	3.23	1.46	5.88	1.31	39.92	0.85	1.13	0.19	1.07	0.96	2.47
BX09	0.88	1.47	0.72	1.72	0.07	0.31	1.03	0.20	0.07	1.05	0.48	1.69	0.21	1.12
BX10	1.85	2.75	1.56	1.83	0.46	0.26	0.43	0.94	0.58	0.43	0.46	1.19	0.11	1.04
BX11	1.13	1.71	1.44	1.78	0.31	0.11	0.82	0.61	0.10	0.78	0.47	1.05	0.14	0.56
BX12	0.71	1.01	0.30	0.55	0.31	0.09	0.72	0.29	0.09	0.72	0.29	0.72	0.11	0.57
BX13	1.03	2.76	1.18	2.83	3.94	0.45	1.44	4.39	0.27	1.29	0.52	1.13	0.51	4.17
BX14	1.31	3.09	1.08	1.40	0.19	0.10	0.32	0.23	0.11	0.38	0.34	0.67	0.08	0.23
BX15	1.71	1.43	1.28	1.50	0.13	0.40	0.64	0.76	0.82	0.58	0.34	0.81	0.11	0.90
BX16	0.61	0.97	0.22	0.27	0.06	0.13	0.50	0.26	0.21	0.59	0.29	0.71	0.06	0.35
Avg.	1.21	1.80	1.15	1.68	0.84	0.57	0.95	3.57	0.29	0.93	0.38	0.98	0.22	1.23

enrichment or deficiency of light and heavy REEs. High values of $(La/Yb)_n > 1$ reflect the enrichment of heavy rare earths, while low values of $(La/Yb)_n < 1$ are a deficit, while the two values of $(La/Sm)_n$ and $(Gd/Yb)_n$ reflect the fractionation of light and heavy rare earths, with higher values indicating a higher degree of fractionation (Hoyle et al., 1984). The $(La/Yb)_n$, $(La/Sm)_n$, and $(Gd/Yb)_n$ of the Benxi Formation shale ranges from 6.41 to 36.54 (average 13.70), 2.45−8.87 (average 5.06), and 0.73−2.98 (average 1.83), respectively, all indicating relatively high fractionation of light and heavy rare earths (Table 5). After normalized by chondrite, the distribution model of

Table 5 Rare earth element characteristics in shale samples (ppm)

Sample ID	La	Ce	Pr	Nd	Sm	Eu	Gd	Tb	Dy	Ho	Er	Tm	Yb	Lu	ΣREE	ΣLREE	ΣHREE	ΣLREE/ΣHREE	$(Gd/Yb)_n$	$(La/Yb)_n$	$(La/Sm)_n$
BX01	58.85	100.71	11.75	45.57	7.56	1.69	6.47	0.95	5.24	1.14	3.29	0.48	2.96	0.45	247.10	226.13	20.97	10.78	1.77	13.48	5.02
BX02	48.01	76.51	9.67	36.11	4.74	0.80	4.17	0.92	6.95	1.62	4.79	0.75	4.6	0.68	200.32	175.85	24.48	7.18	0.73	7.07	6.53
BX03	90.94	147.84	18.37	71.56	12.48	2.31	11.58	1.96	11.89	2.5	7.45	1.21	7.59	1.14	388.8	343.49	45.30	7.58	1.23	8.11	4.70
BX04	85.47	143.15	17.48	68.63	12.81	2.47	12.47	2.20	13.93	3.08	8.85	1.43	9.21	1.37	382.55	330.01	52.53	6.28	1.09	6.29	4.30
BX05	81.95	141.67	15.65	56.98	8.35	1.21	6.25	0.95	6.29	1.42	4.57	0.81	5.07	0.72	331.88	305.81	26.07	11.73	1.00	10.95	6.33
BX06	58.13	101.76	12.08	47.08	8.56	1.71	7.39	1.10	6.11	1.25	3.5	0.56	3.25	0.51	252.98	229.32	23.66	9.69	1.84	12.13	4.38
BX07	34.71	61.46	7.30	28.66	4.86	1.06	4.69	0.68	3.52	0.66	1.92	0.25	1.43	0.22	151.44	138.06	13.38	10.32	2.65	16.43	4.61
BX08	12.81	19.24	2.35	8.91	1.48	0.35	1.45	0.23	1.35	0.3	0.9	0.14	0.85	0.13	50.48	45.13	5.34	8.45	1.38	10.2	5.58
BX09	134.41	273.43	26.59	114.45	21.72	3.11	16.32	2.42	12.65	2.37	6.38	0.97	5.79	0.89	621.49	573.70	47.79	12.01	2.28	15.73	3.99
BX10	54.07	93.43	11.03	44.28	8.09	1.63	7.20	1.05	5.57	1.13	3.01	0.46	2.83	0.42	234.19	212.52	21.67	9.81	2.06	12.96	4.31
BX11	62.07	90.30	12.50	47.11	7.41	1.38	5.89	0.91	5.10	1.02	2.9	0.46	2.73	0.40	240.17	220.77	19.4	11.38	1.74	15.42	5.40
BX12	77.46	120.88	15.02	55.74	10.18	1.92	8.81	1.38	7.43	1.36	3.62	0.54	3.08	0.45	307.86	281.19	26.66	10.55	2.31	17.02	4.91
BX13	60.77	113.17	16.05	72.89	16.00	3.62	15.31	2.57	14.23	2.69	6.95	1.04	6.43	0.99	332.69	282.50	50.19	5.63	1.92	6.41	2.45
BX14	69.10	100.96	11.61	39.04	5.03	1.00	4.37	0.59	2.94	0.53	1.47	0.23	1.28	0.21	238.35	226.73	11.62	19.52	2.76	36.54	8.87
BX15	73.05	119.43	14.77	56.68	9.80	2.18	9.31	1.31	6.80	1.22	3.06	0.44	2.52	0.39	300.95	275.9	25.05	11.01	2.98	19.61	4.81
BX16	24.04	43.04	5.21	19.40	3.29	0.53	2.81	0.53	3.20	0.63	1.76	0.26	1.50	0.21	106.40	95.50	10.90	8.77	1.51	10.83	4.72
Avg.	64.11	109.19	12.96	50.82	8.90	1.68	7.78	1.23	7.07	1.43	4.03	0.63	3.82	0.57	274.23	247.66	26.56	10.04	1.51	10.83	4.72
Chondrite	0.31	0.81	0.12	0.60	0.20	0.07	0.26	0.05	0.32	0.07	0.21	0.03	0.21	0.03	3.29	2.11	1.18	1.79	1.00	1.00	1.00
UCC	30.00	64.00	7.10	26.00	4.50	0.88	3.80	0.64	3.50	0.80	2.30	0.33	2.20	0.32	146.37	132.48	13.89	9.54	1.40	9.24	4.30
NASC	32.00	73.00	7.90	33.00	5.70	1.24	5.20	0.85	5.80	1.04	3.40	0.50	3.10	0.48	173.21	152.84	20.37	7.50	1.35	6.99	3.62

Notes: a) ∑REE = LREE + HREE; b) LREE = La + Ce + Pr + Nd + Sm + Eu; c) HREE = Gd + Tb + Dy + Ho + Er + Tm + Yb + Lu;L/H = LREE/HREE; d) $(La/Yb)_n$, $(La/Sm)_n$, $(Gd/Yb)_n$: subscripts n presents chondrite-normalized value (Taylor and McLennan, 1995).

REEs in the shale samples of the study area showed a right-sloping trend for LREEs and a flattening trend for HREEs (Fig. 2(c)).

5 Discussion

5.1 Palaeo-depositional environment of the Benxi Formation

5.1.1 Depositional site, palaeodepth, and material source

The aqueous environment of the deposition site is important for the preservation and production of organic matter in shale. The $Al_2O_3/(Al_2O_3 + TFe_2O_3)$ values of oceanic ridges, ocean basins, and land margins are < 0.4, 0.4−0.7, and 0.7−0.9, respectively (Roser and Korsch, 1986). The $Al_2O_3/(Al_2O_3 + TFe_2O_3)$ of the Benxi Formation ranges from 0.41 to 0.97 (mean 0.80), indicating that the Benxi Formation was deposited mainly on the terrestrial margin (Table 6) (Roser and Korsch, 1986; Khaled et al., 2022). The La-Th-Sc diagram and ratio of K_2O/Na_2O to SiO_2 can be used to create a discriminant map of depositional sites. The La-Th-Sc diagram shows that most of the samples are located in or near the active continental arc and passive-active continental arc margin regions (Fig. 3(b)). The K_2O/Na_2O-to-SiO_2 ratio discrimination plot shows that the vast majority of the samples are located in passive continental environments (Fig. 3(c)). Both results are consistent with the $Al_2O_3/(Al_2O_3 + TFe_2O_3)$ ratio results, indicating that the Benxi Formation Shale was deposited on a passive continental margin. In this paper, the shale data from the Yichuan area and the Benxi Formation of the Gaoqiao area in the southern Ordos Basin were selected for comparison with the present study. Figure 3(b) shows that the depositional position of the Yichuan area is mainly located in the continental arc, while the main depositional position of the Gaoqiao area is consistent with the present test results, with most samples falling into or adjacent to the active continental arc and passive active continental arc margin areas (Hu et al., 2022).

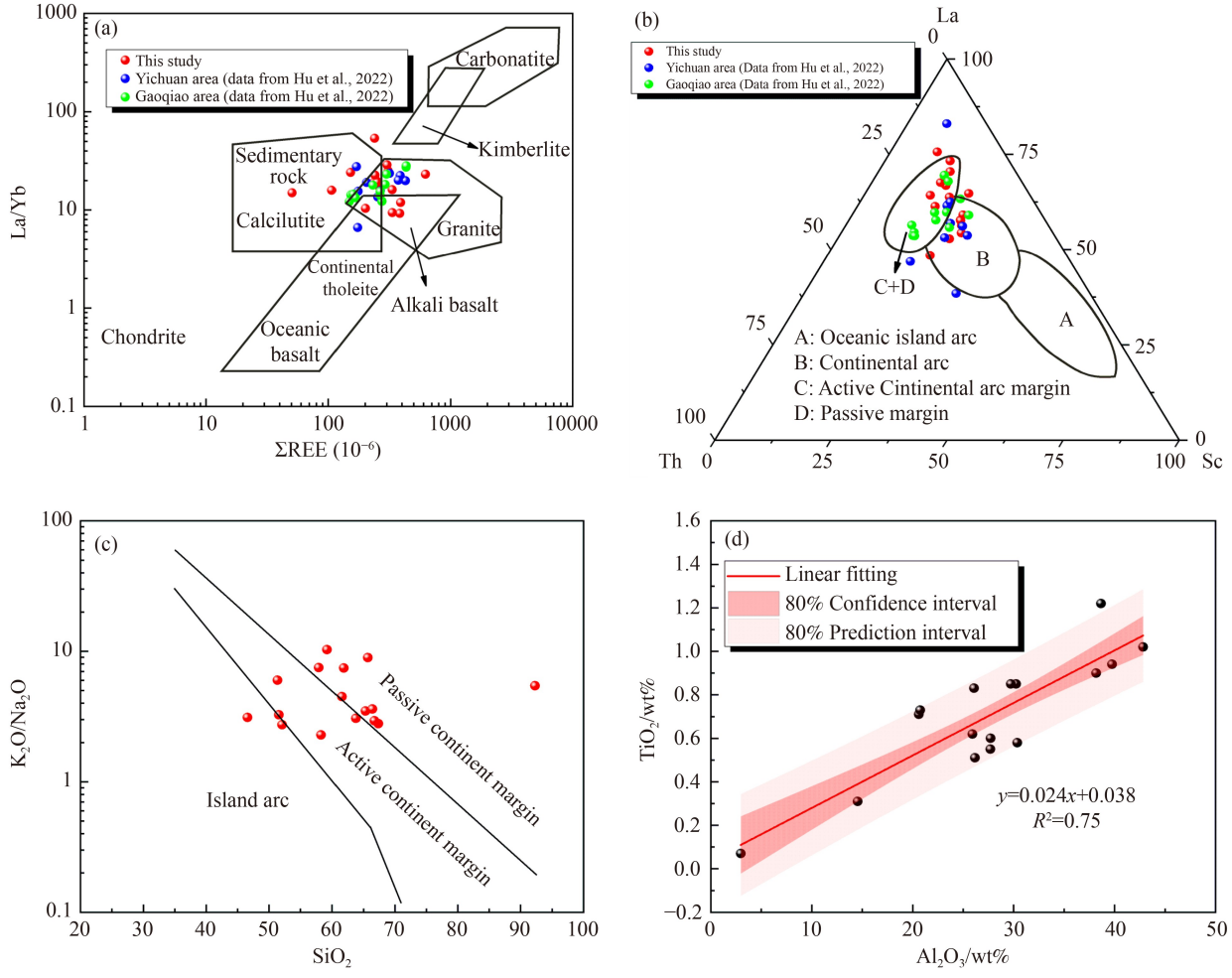

Fig. 3 (a) Source map of shale sediments of the Benxi Formation. (b)−(c) The tectonic background map, blue and green points are from Hu et al. (2022). (d) Discriminant diagram of terrestrial clastic input.

The stability of manganese (Mn), Ferrum (Fe), and titanium (Ti) elements in sediment transport varies. In general, smaller Mn/Fe and Mn/Ti ratios reflect shallow palaeowater depths (Wang et al., 2020). Mn/Fe and Mn/Ti ratios for the shale samples ranged from 0.002 to 0.189 (mean 0.017) and 0.007−8.853 (mean 0.631), respectively, which are low and indicate relatively shallow palaeowater depths during this period at the continental margin and a marine-continental transitional depositional environment (Table 6).

The clastic composition reflects the area of origin, stripping, and transport and controls the hydrocarbon potential of the shale, and the cross-plot of ∑REE and La/Yb can be used as a common indicator of sediment origin (Floyd and Leveridge, 1987). The majority of shale samples from the study area fall into granite and sedimentary rock areas, and most of the Benxi Formation samples in the Yichuan and Gaoqiao areas were also obtained from granite and sedimentary rock areas (Fig. 3(a)). This suggests that the source rocks of the shale of the Benxi Formation are granites and sedimentary rocks of the upper crust, consistent with the source rocks of the Yichuan and Gaoqiao areas in the southern part of the Benxi Formation studied by previous authors. The Y/Ho ratio is often used to reduce the origin of detrital material in the sediment. These values are about 28 for terrestrial clastic rocks and 44−74 for marine chemical sediments. The Y/Ho ratios of the present study range from 23.55 to 32.25 (mean 27.20; Table 6), indicating that the Benxi Formation sediments are dominated by terrestrial clastic rocks (Xu et al., 2014). Metallic elements such as Titanium (Ti) and Aluminum (Al) are often used as indicators to assess the extent of surface clastic flux (Hatch and Leventhal, 1992; Zhao et al., 2021). The TiO_2 and Al_2O_3 contents of the Benxi Formation shale range from 0.07% to 1.22% and 2.97%−39.76%, averages of 0.71% and 27.64% (Table 2), respectively, which are greater than the UCC standard values (0.64% and 15.40%, respectively) and close to the TiO_2 (1.00) and Al_2O_3 (18.90) contents of the PAAS, indicating that the Benxi Formation shale has a high clastic input. TiO_2 has a high positive correlation with Al_2O_3 (R^2 = 0.75; Fig. 3(d)), indicating that the titanium (Ti) in Benxi Formation shale mainly comes from terrestrial clastic material, further implying that the deposition of these shales was accompanied by strong terrestrial clastic input.

5.1.2 Palaeoclimate

Previous studies have shown that palaeoclimate influences to some extent the intensity of chemical weathering and debris influx, which in turn influences the mineralogy and chemical composition of the sediments. Nesbitt and Young (1982) put forward an erratics index ($CIA = Al_2O_3/(A1_2O_3 + CaO^* + Na_2O + K_2O) \times 100$) for the evaluation of palaeoclimatic changes. CaO in silicates as CaO* and is corrected by the expression $CaO^* = CaO - (10/3 \times P_2O_5)$. The result is taken as the difference between CaO* and Na_2O content the smaller value (Nesbitt and Young, 1982). 50 < CIA < 70, 70 < CIA < 85, and 85 < CIA < 100 indicate cold and dry, warm and humid, and hot and humid climates, respectively, and the degree of chemical weathering gradually increases with the CIA value (Nesbitt and Young, 1982; Li et al., 2019c). The Index of Constituent Variability (ICV) is commonly used to represent sediment recycling and is a prerequisite for the CIA. $ICV = (Fe_2O_3 + K_2O + Na_2O + CaO^* + MgO + MnO + TiO_2)/Al_2O_3$, with ICV > 1.0 indicating that deposition occurred during a tectonically active period and that the sediments contain small amounts of clay minerals. Meanwhile ICV < 1.0 indicate that debris was redeposited or deposited under strong weathering conditions, at which point the CIA is indicative of the degree of chemical weathering (Fedo et al., 1995; Cullers and Podkovyrov, 2002). The ICV of the Benxi Formation ranges from 0.12 to 3.04 (mean 0.61) and the CIA ranges from 78.56 to 95.28 (mean 90.34), this indicates that the climate was hot and humid during the deposition of the Benxi Formation shale in the study area, with strong chemical alteration (Table 6). The relative contents of some climate-sensitive trace elements are often used to restore paleoclimate, of which C_{value} is a common indicator, where $C_{value} = \sum(Fe + Mn + Cr + Ni + V + Co)/\sum(Ca + Mg + Sr + Ba + K + Na)$. $C_{value} > 0.8$, $0.2 < C_{value} < 0.8$, $C_{value} < 0.2$ for humid climate, semi-arid to semi-humid climate, and arid climate, respectively (Awan et al., 2020; Wu et al., 2022a). The C_{value} of the Benxi Formation shale ranges from 0.29 to 4.97 (mean 1.91), indicating that the Benxi Formation shale was deposited in a humid environment, which is similar to the results measured by the CIA parameters (Table 6).

5.1.3 Redox conditions

Sedimentary rocks vary in their enrichment of trace elements under different redox conditions, and previous authors have commonly used U/Th and Ni/Co to reduce the redox conditions of the sedimentary environment (Tribovillard et al., 2006; Jenkyns et al., 2017; Shi et al., 2022). Common redox condition proxies and discrimination criteria are shown in Table 7. The mean values of five parameters of the Benxi Formation, Ni/Co, U/Th, δU, V/(V + Ni), and Ce/La are 3.08, 0.44, 0.98, 0.71, and 1.68, respectively, indicating that the Benxi Formation shale depositional environment as a whole exhibits a depleted oxygen reduction state (Table 7). The cerium anomaly index (Ce_{anom}) can be used as a marker to judge the redox conditions of the palaeoaqueous medium, where $Ce_{anom} = Log_{10}[3Ce_n/(2La_n + Nd_n)]$ (n represents the standardization of Post-Archean Australian Shale). When $Ce_{anom} > -0.1$ indicates a Cerium (Ce) enriched,

Table 6 Common palaeoenvironmental indicator parameters for shale samples

Sample ID	$Al_2O_3/(Al_2O_3+TFe_2O_3)$	Mn/Fe	Mn/Ti	Y/Ho	CIA	ICV	C_{value}	Ni/Co	U/Th	δU	V/(V + Ni)	Ce/La	Ce_{anom}	Sr/Ba	Th/U	*m*	P/Ti	Fe/Ti	(Fe + Mn)/Ti	$(La/Yb)_N$	Mo/TOC
BX01	0.80	0.005	0.065	25.76	91.82	0.38	1.94	1.62	0.34	1.01	0.80	1.71	−0.05	0.66	2.97	1.98	0.07	13.24	13.31	1.77	1.25
BX02	0.97	0.004	0.007	27.62	93.16	0.15	0.29	3.46	0.24	0.83	0.85	1.59	−0.08	0.94	4.25	1.81	0.02	1.79	1.80	0.73	0.57
BX03	0.93	0.003	0.014	30.26	93.84	0.18	0.78	3.95	0.47	1.17	0.62	1.63	−0.07	1.19	2.15	1.77	0.03	4.20	4.21	1.23	0.63
BX04	0.79	0.002	0.035	29.65	93.33	0.39	2.64	3.94	0.55	1.24	0.55	1.67	−0.06	1.16	1.83	2.03	0.03	16.13	16.16	1.09	0.42
BX05	0.94	0.005	0.015	25.42	89.93	0.23	0.44	3.61	0.47	1.17	0.88	1.73	−0.03	0.77	2.14	1.96	0.02	3.19	3.20	1.00	0.73
BX06	0.84	0.006	0.056	27.76	83.75	0.46	0.71	1.79	0.26	0.88	0.83	1.75	−0.04	0.37	3.85	4.05	0.12	9.50	9.56	1.84	0.87
BX07	0.68	0.002	0.038	24.57	92.92	0.60	3.51	1.70	0.28	0.91	0.63	1.77	−0.04	0.6	3.59	1.6	0.03	15.87	15.91	2.65	9.93
BX08	0.51	0.189	8.853	34.92	88.92	1.58	2.20	3.66	1.84	1.69	0.57	1.50	−0.09	3.71	0.54	22.56	1.32	46.83	55.69	1.38	1.17
BX09	0.78	0.011	0.155	25.8	95.16	0.38	2.88	4.78	0.25	0.86	0.61	2.03	0.01	2.39	4.01	2.57	0.12	13.68	13.83	2.28	0.39
BX10	0.71	0.010	0.140	27.13	88.33	0.64	1.96	2.35	0.20	0.75	0.75	1.73	−0.05	0.29	5.05	5.16	0.08	13.74	13.88	2.06	0.82
BX11	0.77	0.001	0.012	23.75	95.76	0.38	4.97	2.46	0.28	0.92	0.66	1.45	−0.12	0.69	3.54	0.76	0.02	12.24	12.26	1.74	0.36
BX12	0.96	0.006	0.011	25.44	95.88	0.12	0.67	3.69	0.32	0.98	0.8	1.56	−0.08	0.60	3.13	0.82	0.03	1.93	1.94	2.31	0.39
BX13	0.41	0.008	0.633	32.25	87.44	1.63	4.13	4.82	0.92	1.47	0.52	1.86	−0.08	1.07	1.09	3.71	1.13	78.08	77.45	1.92	1.54
BX14	0.87	0.002	0.013	23.68	95.08	0.25	2.23	2.59	0.24	0.85	0.74	1.46	−0.08	0.57	4.08	0.98	0.01	5.75	5.76	2.76	1.09
BX15	0.8	0.004	0.036	27.68	78.96	0.60	0.71	2.34	0.27	0.89	0.77	1.63	−0.07	0.31	3.72	3.87	0.10	9.39	9.43	2.98	1.75
BX16	0.97	0.015	0.018	23.55	95.17	0.13	0.45	2.43	0.16	0.65	0.87	1.79	−0.03	0.39	6.18	0.91	0.01	1.21	1.23	1.51	0.17
Avg.	0.80	0.017	0.631	27.20	91.22	0.51	1.91	3.07	0.44	1.02	0.72	1.68	−0.06	0.98	3.26	3.53	0.20	15.38	16.02	1.83	1.38

Table 7 The proxies of redox conditions and discrimination criteria

Redox conditions	Oxic	Dysoxic	Anoxic	Ref.	Sample mean	Sample Redox
Ni/Co	<2.5	2.5−5	>5	Jones and Manning (1994)	3.07	Dysoxic
U/Th	<0.27	0.27−0.5	>0.5	Dypvik and Harris (2001)	0.44	Dysoxic
δU	<1	>1		Liang et al. (2020)	1.02	Dysoxic
V/(V + Ni)	<0.57	0.57−0.83	>0.83	Hu et al. (2018)	0.72	Dysoxic
Ce/La	>1.8	1.5−1.8	<1.5	Wu et al. (2022a)	1.68	Dysoxic
Ce_{anom}	<−0.1	>−0.1		Elderfield and Greaves (1982)	−0.06	Dysoxic

a) δU = 2U/(U + Th/3).

anoxic reducing environment, while Ce_{anom} < −0.1 indicates a Cerium (Ce) deficit, reflecting an oxygen-rich oxidizing environment in the water column (Elderfield and Greaves, 1982). The Ce_{anom} of the Benxi Formation shale is −0.12−0.01 (mean −0.06), indicating a depositional environment dominated by reducing conditions (Table 7).

5.1.4 Palaeosalinity

Palaeosalinity determination can be used to identify the extent and duration of seawater intrusion, analyze sedimentary facies zones and characterize the depositional environment (Abanda and Hannigan, 2006). The ratio of Strontium (Sr) and Barium (Ba), as elements that are more sensitive to the salinity of the water column, is a more common indicator of paleosalinity (Meng et al., 2012; Chen et al., 2020). In fine-grained sedimentary rocks of terrestrial origin, potassium feldspar and black mica act as carriers to elemental Barium (Ba), which is relatively enriched, while the marine sedimentary environment is more favorable to Strontium (Sr) enrichment, which is due to the similar radii of Strontium ion (Sr^{2+}) and Calcium ion (Ca^{2+}). In Ca-rich carbonate rocks, Strontium ion (Sr^{2+}) similarly replaces Calcium ion (Ca^{2+}), resulting in Strontium (Sr) enrichment, and the higher the Sr/Ba ratio, the greater the palaeosalinity. Typically, the deposition environment is identified as saline water environment when Sr/Ba > 1, semi-saline water environment when 0.5 < Sr/Ba < 1, and freshwater environment when Sr/Ba < 0.5 (Stüben et al., 2002; Zhang et al., 2018b). Shale Sr/Ba of the Benxi Formation between 0.29 and 3.71 (mean 0.98), indicating overall high palaeosalinity and a semi-saline environment during deposition of the Benxi Formation shale (Table 6). Th/U values can often be used to identify shale depositional environments. In general, Th/U > 7, 2 < Th/U < 7, and Th/U < 2 indicate terrestrial freshwater environments, brackish-saline sedimentary environments, and marine brackish environments respectively (Zhang et al., 2008). Th/U values of Benxi shale are between 0.54 and 6.18 (mean 3.26), further demonstrating that the Benxi Formation has high palaeosalinity and was in a semi-saline depositional environment (Table 6). The ratio of the content of MgO in sedimentary rocks can be used to discern the palaeosalinity of water bodies, which is usually calculated by $m = 100 \times (MgO)/(Al_2O_3)$. Freshwater depositional environments are indicated by $m < 1$, marine-continental transitional depositional environments by $m = 1−10$, and seawater depositional environments by $m > 10$ (Guo, 2020). The m values of the Benxi Formation shale range from 0.76 to 22.56 (mean 3.53; Table 6), indicating that the salinity of the water column was high during the deposition of the shale in the Benxi Formation, consistent with the results measured for both Sr/Ba and Th/U.

5.1.5 Palaeoproductivity and volcanic hydrothermal fluid

Palaeoproductivity is often defined as the rate at which ancient marine organisms fix energy during the energy cycle. A sedimentary environment with high palaeoproductivity not only provides a large amount of organic matter, but this organic matter can consume oxygen in the water column, thus further creating an anoxic reduction environment that is conducive to the preservation of organic matter (Bernárdez et al., 2008; Stock et al.,2017). The P/Ti can be used as a geochemical indicator of palaeoproductivity. Phosphorus (P) is an important planktonic nutrient and is the element limiting palaeoproductivity, so phosphorus in sediments is often used as a proxy for palaeoproductivity (Latimer and Filippelli, 2002). Benxi Formation shale with P/Ti of 0.01−1.3 (mean 0.20; Table 6), which is higher than those of the PAAS (0.12) and UCC (0.17), indicating high palaeoproductivity of the Benxi Formation during the depositional period (Taylor and McLennan, 1985). In recent years, numerous studies have confirmed that TOC is associated with Molybdenum (Mo) content in organic-rich sediments, and Molybdenum (Mo) content can be used to reflect the magnitude of palaeoproductivity (Algeo and Tribovillard, 2009). The Benxi Formation shale has a Molybdenum (Mo) content of 0.75×10^{-6}−13.11×10^{-6} (mean 3.35×10^{-6}; Table 3), which is greater than the PAAS standard value of 1.0×10^{-6}. Both indicators suggest a high level of palaeoproductivity during its depositional period. It is known from previous experience that the main body of the shale of the Benxi

Formation in the Ordos Basin is Type III organic matter derived from higher plants, and the high P/Ti values of the shale of the Benxi Formation suggest that large amounts of plankton were also present in their deposition (Li et al., 2019c; Chen et al., 2020; Yang et al., 2022).

Volcanic hydrothermal fluid is rich in nutrients and can increase water temperatures, providing good conditions for the flourishing of biological communities such as bacteria and algae. Thus, hydrothermal fluid enhances biological productivity (Qi et al., 2004; Chen et al., 2021). The hydrothermal environment favors the deposition of Ferrum (Fe) and Manganese (Mn), while high values of Titanium (Ti) may reflect terrestrial input. Fe/Ti and (Fe + Mn)/Ti values are widely used indicators of hydrothermal sources, when Fe/Ti > 20 or (Fe + Mn)/Ti > 25 ± 5, the deposit is usually considered to be influenced by hydrothermal fluid (Yamamoto, 1987; Ma et al., 2019; He et al., 2022). The Fe/Ti and (Fe + Mn)/Ti values of the Benxi Formation shale range from 1.21 to 77.45 (mean 15.38) and 0.23 to 78.08 (mean 16.02), respectively (Table 6), indicating that the Benxi Formation sediments were deposited without an obvious influence from volcanic hydrothermal fluids. However, it is noteworthy that the Fe/Ti and (Fe + Mn)/Ti values of samples BX08 and BX13 are higher than the standard values, indicating local volcanic hydrothermal fluid during the deposition of the Benxi Formation shale.

5.1.6 Sedimentation rate and stagnation environment

The shale organic enrichment process is more significantly influenced by the sedimentation rate. A higher sedimentation rate can reduce the degree of rare earth differentiation. At lower sedimentation rates, the differentiation of light and heavy rare earths is stronger, and rare earth and organic matter are adsorbed by clays and other materials, while too high sedimentation rates have a dilutive effect on organic matter (Tyson, 2001; Tenger et al., 2006). $(La/Yb)_N$ is a parameter used for evaluating the sedimentation rate of shales. When $(La/Yb)_N$ is similar to 1, it indicates a high sedimentation rate and low rare earth differentiation, and When the difference between $(La/Yb)_N$ values compared to 1 is large, it indicates a low shale deposition rate and high rare earth differentiation, the subscript N represents the standardization of NASC (Doner et al., 2019). The $(La/Yb)_N$ distribution of the shale samples ranges from 0.73 to 2.98 (mean 1.83; Table 5), indicating a high deposition rate and low rare earth differentiation in the Benxi Formation shale.

In stagnant deepwater environments, bacterial sulfate-reducing environments form hydrogen sulfide, which enriches Mo in the sediments while depleting it from seawater. Three types of stagnation environment can be derived from previous experience, Mo/TOC < 4.5, 4.5 < Mo/TOC < 45 and Mo/TOC > 45 representing strong, semi-stagnation and weak stagnation environment, respectively (Algeo and Rowe, 2012). The Mo/TOC of Benxi Formation shale samples ranges from 0.36 to 9.93 (mean 1.31; Table 6), indicating deposition in a strong stagnant environment. This is consistent with the report of a stagnant environment for the Benxi Formation shale in the Zhaoxian section and well M115 of Linxian, Shanxi, eastern Ordos Basin (Fig. 4) (Cui et al. 2022).

5.2 Organic matter enrichment mode of the Benxi Formation shale

It is clear from the above that the shale of the Benxi Formation was deposited in a hot and humid climate with high palaeoproductivity and local volcanic hydrothermal fluid, accompanied by strong terrestrial clastic input and a high sedimentation rate and stagnation degree. The bottom water as a whole was in oxygen-poor reducing conditions and a semi-saline deposition environment. The organic matter enrichment of shale is influenced by multiple factors. The palaeoenvironment (palaeoclimate, redox conditions, palaeosalinity, etc.) is a fundamental factor influencing the diversity, growth, and decomposition of organisms, controlling the production and preservation of organic matter (Talbot, 1988; Chen et al., 2019). To determine which or which factors control their organic enrichment, this study used TOC to represent the degree of organic matter enrichment and analyzed its relationships with terrestrial clastic input indicators (Aluminum (Al), Titanium (Ti), Thorium (Th)), palaeoproductivity indicators (P/Ti, Molybdenum (Mo)), volcanic hydrothermal fluid indicators (Fe/Ti, (Fe + Mn)/Ti), palaeoclimatic indicators (CIA, C_{value}), water body redox condition indicators (U/Th, δU), palaeosalinity indicators (Sr/Ba, m (m = 100 × (MgO)/(Al_2O_3)),

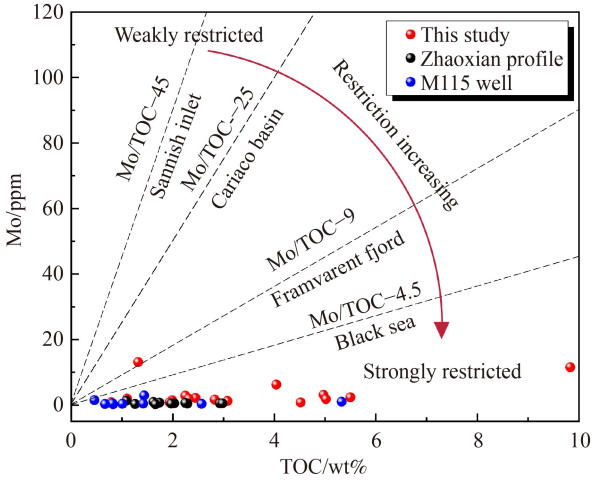

Fig. 4 Stagnant environment discrimination diagram of the Benxi Formation shale, with data from the Zhaoxian section and M115 well from Cui et al. (2022).

sedimentation rate indicators ($(La/Yb)_N$) and stagnant environment indicators (Mo/TOC).

Terrestrial clastic and sedimentation rate are important factors affecting organic matter enrichment. Terrestrial clastic input can transport terrestrial organic matter into water and enrich organic matter accumulation. However, excessive input of terrestrial-sourced debris material can have a diluting effect on productivity. Aluminum (Al), Titanium (Ti), and Thorium (Th) elements are often used to indicate the degree of influence of clastic input from terrestrial sources (Tyson, 2001; Ding et al., 2015). Aluminum (Al), Titanium (Ti), and Thorium (Th) elements of the Benxi Formation shale samples all show negative correlations with TOC (R^2 = 0.36, 0.51, and 0.13, respectively; Fig. 5(a)). The influx of detritus provides abundant organic matter (plant decomposition) on the one hand, and acts as a diluent of organic matter, on the other hand, indicating that the excessive terrestrial detrital material infusion has a dilution effect while providing sufficient organic matter, and the dilution effect exceeds its organic matter supply. Thus, the terrestrial clastic is not an influencing factor for its organic matter enrichment. The sedimentation rate indicators ($(La/Yb)_N$) are not significantly correlated with the terrestrial clastic input indicators (Aluminum (Al), Titanium (Ti), Thorium (Th)) and is weakly correlated with TOC, while the stagnant environment indicators (Mo/TOC) are weakly negatively correlated with TOC (R^2 = 0.25; Figs. 5(b)−(c)). This suggests that the input of terrestrial clastic from the Benxi Formation shale is independent of the sedimentation rate and that both sedimentation rate and sedimentation rate have a weak influence on shale organic matter enrichment.

The palaeoclimatic indicators (CIA, C_{value}) of the Benxi Formation shale correlate extremely weakly with TOC (Fig. 5(d)), suggesting that hot and humid climatic conditions do not play a significant role in promoting biological growth and reproduction, therefore palaeoclimate is not the main controlling factor for organic matter enrichment in the Benxi Formation shale. This trend differs from those reported for the Shanxi Formation and Longtan Formation of the marine-continental transitional facies (Liu et al., 2018; Wei et al., 2020), which indicates that under equally humid conditions, excessive temperatures could probably inhibit organic enrichment in the shale of the Benxi Formation.

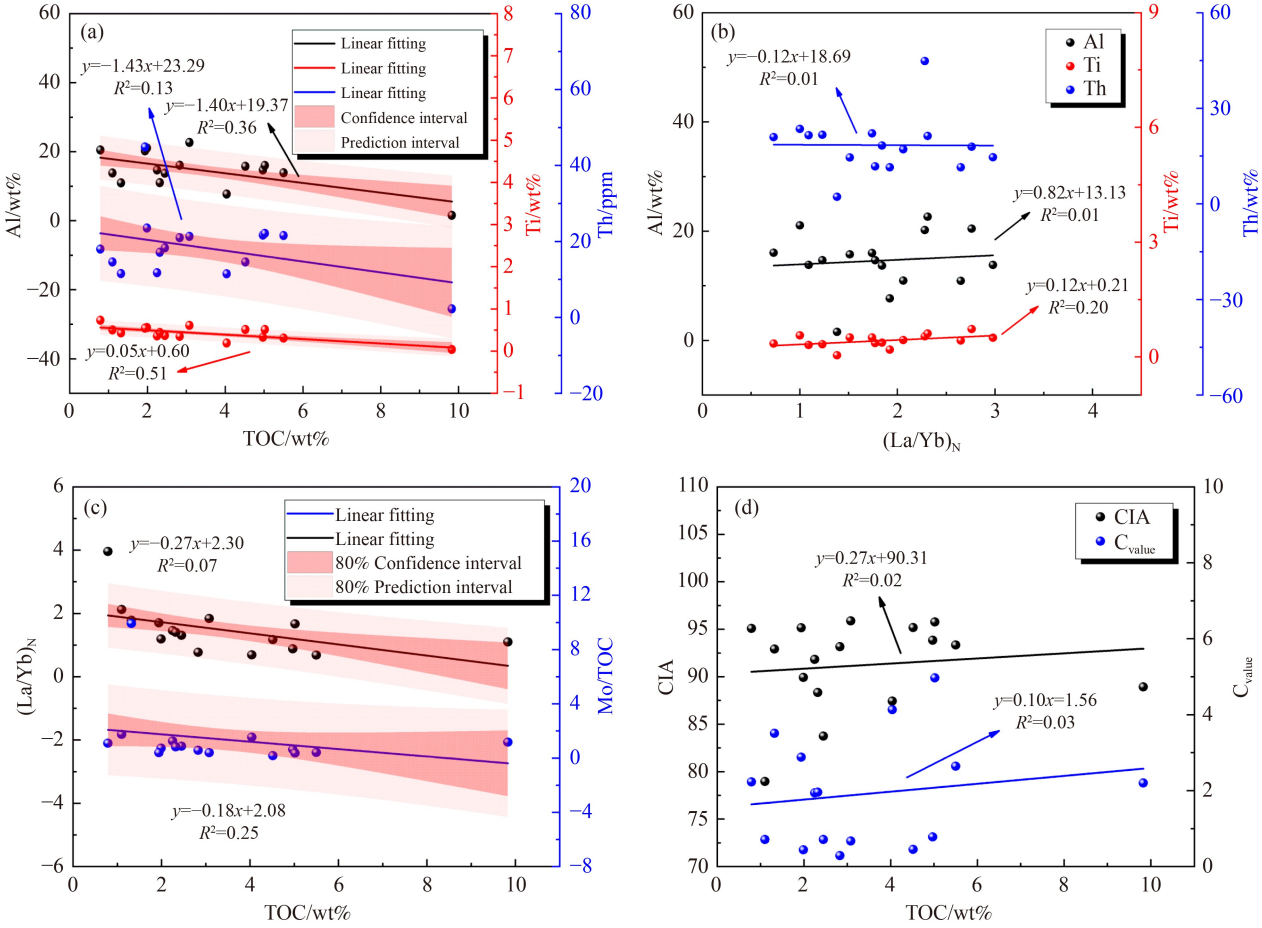

Fig. 5 Correlation analysis of terrestrial clastic input indicators with (a) TOC; (b) Sedimentation rate indicators; Correlation analysis of TOC with (c) Sedimentation rate and stagnant environment indicators; (d) Palaeoclimate indicators.

The TOC of the Benxi Formation shale is positively correlated with the P/Ti ratio and Molybdenum (Mo) content (R^2 = 0.39 and 0.14, respectively; Fig. 6(a)), indicating that higher palaeoproductivity provided a certain material basis for the organic matter enrichment during the deposition of the shales in the Benxi Formation and that palaeoproductivity is one of the influences on the organic-rich shale. This trend is consistent with previous reports on Carboniferous-Permian marine-continental transitional facies rocks of Ordos Basin (Wei et al., 2020; Zhang et al., 2021). In this study, the TOC content was weakly positively correlated with (Fe + Mn)/Ti and Fe/Ti (R^2 = 0.18 and 0.27, respectively; Fig. 6(b)), indicating that local volcanic hydrothermal fluid provided certain nutrients to Benxi Formation shale and elevated water temperatures, which could provide better conditions for biological communities such as mycorrhizal algae and, in turn, promote organic matter enrichment.

The palaeowater depth indicators (Mn/Fe, Mn/Ti) and redox condition indicators U/Th of the Benxi Formation shale are significantly positively correlated (R^2 = 0.79 and 0.84, respectively; Fig. 7(a)) and the water body redox condition indicators (U/Th, δU) show a strong correlation with TOC (R^2 = 0.63 and 0.47, respectively; Fig. 7(b)). This indicates that with the deepening of palaeowater, the aqueous reducing conditionality of the Benxi Formation shale was enhanced. The moderate palaeowater depths of the marine-continental transitional shale depositional environment, result in an oxygen-poor reducing aqueous environment. To some extent, the reducing environment occurred between the continental and marine shale, and the oxygen-poor reducing environment favors the preservation of organic matter and promotes organic matter enrichment. It is consistent with the trends of the Niutitang and Longmaxi Formations measured by Li et al. (2019a) and the Shahejie Formation measured by Hu et al. (2018). Currently, redox-sensitive elements (RSEs) enrichments, for instance, Mo and U, can be used to analyze the depositional environment of shales. The Mo_{EF} of the Benxi Formation shale ranges from 0.20 to 39.92 (mean 3.69) and the U_{EF} ranges from 0.44 to 7.57 (mean 1.72), with a high positive correlation between U_{EF} and Mo_{EF} (R^2 = 0.79; Fig. 7(c)). This reveals that Mo and U elements are highly enriched and co-occur, forming in an anoxic-sulfidic deposition environment (Tang et al., 2015). The TOC shows a good positive correlation with both Mo_{EF} and U_{EF} (R^2 = 0.55 and 0.65, respectively; Fig. 7(d)), and multiple indicators suggest that bottom-water anoxic reduction conditions favor organic enrichment in the shales of the Benxi Formation.

The palaeosalinity indicators (Sr/Ba, m (m = 100 × (MgO)/(Al_2O_3))) of the Benxi Formation shale are both proportional to TOC (R^2 = 0.47, 0.49, respectively; Fig. 8), manifesting that higher palaeosalinity has a significant impact on the growth and preservation of palaeontological. The higher salinity water environment favors the preservation of organic matter, which is close to previous work on the organic matter enrichment of transitional shales in the north-eastern Ordos Basin (Chen et al., 2020).

From the above analysis, it is clear that the enrichment of organic matter in the marine-continental transitional shale of the Benxi Formation is the result of the interaction of several factors, such as palaeoproductivity, volcanic hydrothermal fluid, water body redox conditions, and palaeosalinity. All of the above factors directly or indirectly influence the production and preservation of organic matter in shale, further contributing to organic enrichment. Among these factors, redox conditions have the greatest influence, while palaeosalinity and palaeoproductivity promotion are second, and volcanic hydrothermal fluids have a weaker influence (Table 8).

Combined with the above analyses and the regional sedimentary tectonic setting, a organic matter enrichment mode of the Benxi Formation shale can be restored (Fig. 9(a)). These shales are of a marine-continental transitional facies and were deposited on the continental margin. The hot and humid environment during the

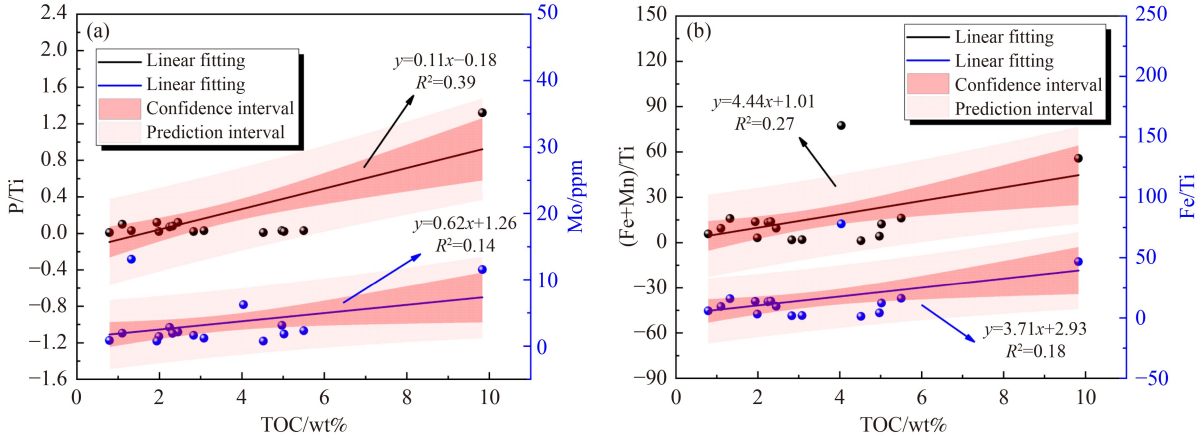

Fig. 6 Correlation analysis between TOC and (a) Palaeoproductivity indicators; (b) Volcanic hydrothermal fluid indicators.

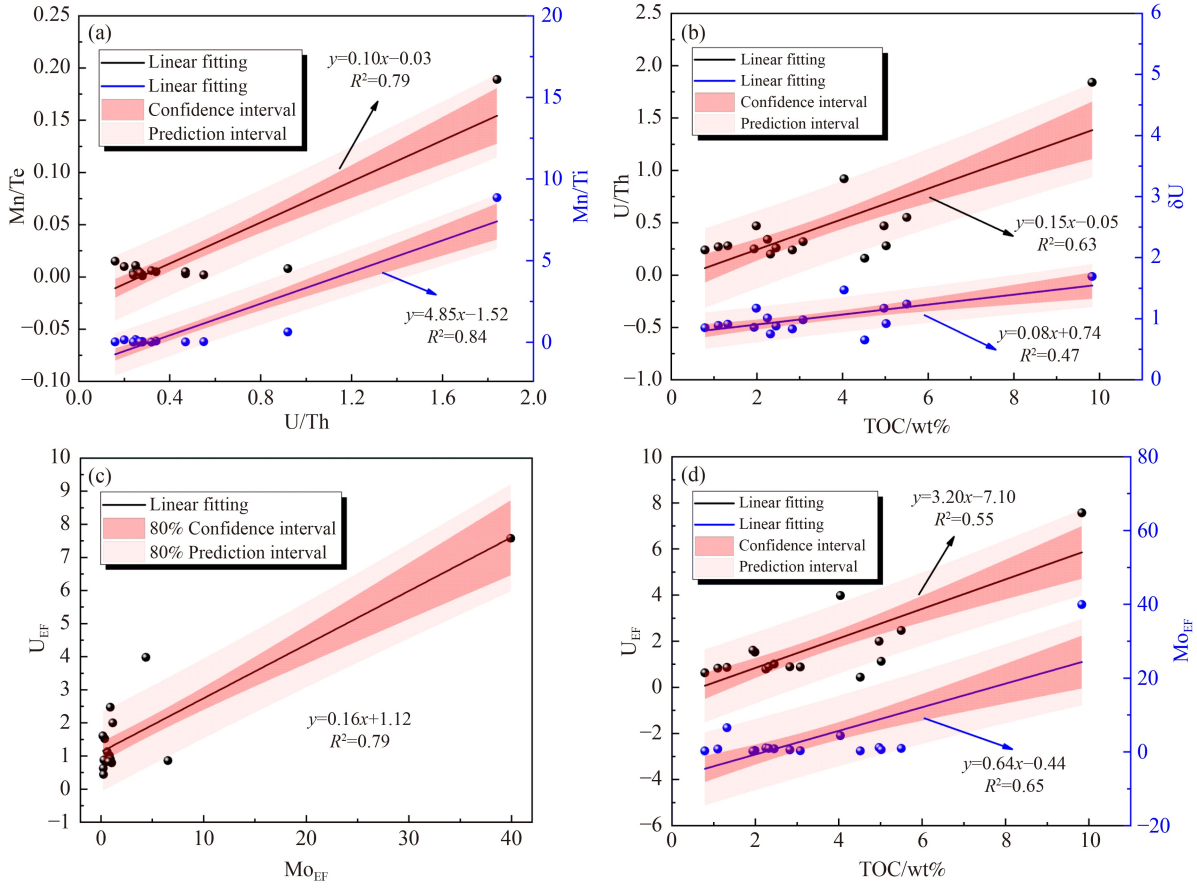

Fig. 7 Correlation analysis of water body redox condition indicators with (a) palaeowater depth indicators; (b) TOC; (c) redox-sensitive element (RSE) enrichment degree Mo_{EF} and U_{EF} correlation analysis; (d) TOC and Mo_{EF} and U_{EF} correlation analysis.

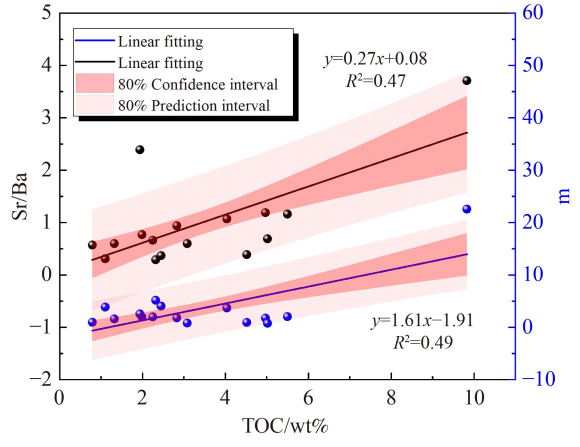

Fig. 8 Correlation analysis of TOC and palaeosalinity indicators.

deposition period promoted biological growth and accelerated rock weathering. Input of terrestrial clastic and local volcanic hydrothermal fluid also promoted biological reproduction, so that the Benxi Formation shale had high palaeoproductivity and formed abundant organic matter. An oxygen-poor and high-salinity bottom-water environment is conducive to organic matter preservation, while biological respiration can increases the consumption of oxygen in the water column. The high sedimentation rate and strong stagnation environment also reduce the time for oxidative decomposition of organic matter in the water column, allowing for rapid deposition and burial and creating a unique mode of organic enrichment in this formation and sedimentary facies.

5.3 Differential enrichment mechanism of organic-rich shale under sedimentary facies

In this study, the geochemical characteristics of organic matter-rich shale under three different sedimentary facies were cited, compared, and analyzed (where the Longtan and Shanxi formations are marine-continental transitional facies, the Chang 7, Chang 9, and Shahejie formations are derived from continental facies, and the Dalong, Sowa, and Niutitang formations are marine facies) (Zeng et al., 2015; Zhang et al., 2017; Chen et al., 2021; Wu et al., 2021; Zhang et al., 2021; Wu et al., 2022b; Xu et al., 2022). The specific parameters are shown in Table 9. Combining their production factors (terrestrial clastic input, palaeoclimate, palaeoproductivity, and volcanic hydrothermal fluid) with preservation factors (redox conditions, palaeosalinity, sedimentation rate, and stagna-

Table 8 Analysis table of the main controlling factors of organic matter enrichment in the shale of the Benxi Formation

Impact factors	Indicators	Impact level	Correlation coefficient
Water body redox	U/Th	Major	R^2 = 0.63, positive
	δU		R^2 = 0.47, positive
	U_{EF}		R^2 = 0.55, positive
	Mo_{EF}		R^2 = 0.65, positive
Palaeosalinity	Sr/Ba	Major	R^2 = 0.47, positive
	m (m = 100 × (MgO)/(Al_2O_3))		R^2 = 0.49, positive
Palaeoproductivity	P/Ti	Minor	R^2 = 0.39, positive
	Molybdenum (Mo)		R^2 = 0.14, positive
Volcanic hydrothermal fluid	Fe/Ti	Minor	R^2 = 0.18, positive
	(Fe + Mn)/Ti		R^2 = 0.27, positive
Terrigenous detrital	Aluminum (Al)	Minor	R^2 = 0.36, negative
	Titanium (Ti)		R^2 = 0.13, negative
	Thorium (Th)		R^2 = 0.51, negative
Stagnant environment	Mo/TOC	Minor	R^2 = 0.25, negative
Palaeoclimatic	CIA	Negligible	R^2 = 0.02, positive
	C_{value}		R^2 = 0.03, positive
Sedimentation rate	$(La/Yb)_N$	Negligible	R^2 = 0.07, negative

tion environment), so the differences in depositional environments and organic matter enrichment mechanisms of shale in three different sedimentary facies are proposed (Figs. 9 and 10).

The organic-rich shale of the continental, marine-continental transitional, and marine facies are often deposited in the semi-deep lacustrine – deep lacustrine, lagoonal, and Shelf sedimentary facies. The marine-continental transitional tidepool-lagoon deposits are located closer to land and are more influenced by the land, with the highest Al_2O_3 and TiO_2 contents among the three. The Al_2O_3 and TiO_2 contents of organic-rich shale under the three sedimentary facies are as follows: marine-continental transitional shale (average of 22.45 wt% and 0.78 wt%) > continental shale (average of 14.23 wt% and 0.49 wt%) > marine shale (average of 8.36 wt% and 0.34 wt%; Table 9, Fig. 10(a)). In terms of paleoclimate (CIA, C_{value}), the values under each depositional facies are as follows: marine-continental transitional shale (average of 86.44 and 0.89) > marine shale (average of 71.64 and 0.42) ≈ continental shale (average of 68.47 and 0.38). This indicates that the main body of the marine-continental transitional shale was deposited in a warm, humid and hot, humid climate with strong chemical weathering, whereas the terrestrial and marine shale deposition environments were in a cold, dry to warm, humid state, but both were dominated by the warm, humid environment (Table 9, Fig. 10(b)). It can be seen that the stronger chemical weathering and warm and humid climatic conditions are more conducive to shale organic matter enrichment. The global climate change curve shows that the palaeoclimate during the deposition of continental and marine shales was in the vicinity of the warm and cold climate divide and the warm region, in agreement with the CIA parameter results(Fig. 10(j)) (Liang et al., 2020). It is important to note that the Carboniferous-Permian period is predominantly located in a cold region and the period as a whole was a major ice age, but global mean temperatures rebounded near the junction of the late Carboniferous and early Permian, and the marine-continental transitional shale in the study area developed mainly during this facies. Previous studies have shown that the southern hemisphere had a cold glacier-covered climate during this period, while the northern hemisphere had a warm and humid tropical and subtropical climate, and northern and southern China were in the northern hemisphere and close to the equator at this time (Fig. 1(a)) (Liang et al., 2020; Scotese et al., 2021; Zhang et al., 2022). So the climate was warm and humid to hot and humid, which is consistent with the results shown by geochemical parameters in this study. This suggests that although the palaeoclimate of organic matter-rich shale in the study area in the marine-continental transitional facies is not consistent with the global mean temperature, it is still an important factor in the enrichment of organic matter in shale (Table 9, Fig. 10(j)). In terms of palaeoproductivity (P/Ti, Molybdenum (Mo)) and volcanic hydrothermal fluid (Fe/Ti, (Fe + Mn)/Ti), the differences between the three sedimentary facies are relatively small, with P/Ti and Molybdenum (Mo) values greater than 0.1 and 1 ppm, respectively, and Fe/Ti and (Fe + Mn)/Ti values both close to 10 on average, with some values greater than 25, indicating that the palaeoproductivity corresponding to

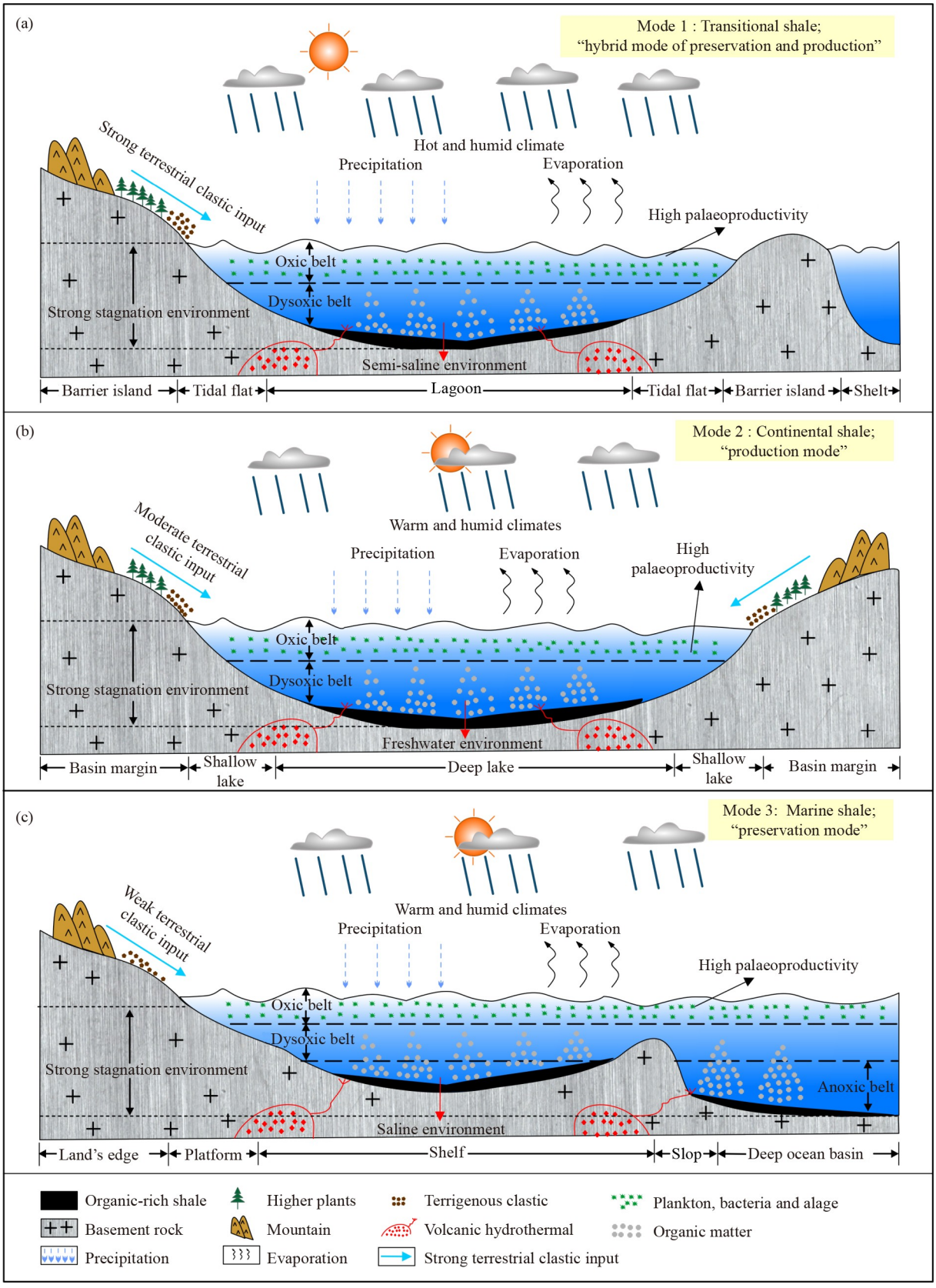

Fig. 9 Organic matter enrichment modes in shale sedimentary facies differences. (a) Marine-continental transitional shale organic matter enrichment mode; (b) continental shale organic matter enrichment mode (modified from Yu et al., 2022); (c) marine shale organic matter enrichment mode (modified from Lan and Shen, 2022).

Table 9 Sedimentary environmental indicators of organic-rich shale in different sedimentary facies and their sources

Sedimentary facies		Marine-continental transitional shale			Continental shale			Marine shale		
Formation		Benxi	Longtan	Shanxi	Chang 7	Chang 9	Shahejie	Dalong	Suowa	Niutitang
Site		Ordos Basin	Yangtze region	Ordos Basin	Ordos Basin	Ordos Basin	Bohai Bay Basin	Yangtze region	northern Tibet	Yangtze
Period		Carboniferous	Permian	Permian	Triassic	Triassic	Paleogene	Permian	Cretaceous	cambrian
Ref.		This study	Wu et al., 2022b	Zhang et al., 2021	Zhang et al., 2017	Chen et al., 2021	Wu et al., 2021	Wu et al., 2022b	Zeng et al., 2015	Xu et al., 2022
TOC (wt%)		0.79–9.83 (3.37)	0.60–2.20 (0.98)	0.83–35.4 (7.32)	5.79–28.27 (17.50)	1.22–11.6 (6.56)	0.33–2.55 (0.99)	1.30–6.40 (2.73)	2.96–23.47 (9.56)	0.49–8.77 (2.81)
Terrigenous detrital	TiO_2	0.07–1.22 (0.71)	0.61–0.94 (0.80)	0.40–1.33 (0.82)	0.21–0.65 (0.46)	0.21–0.65 (0.43)	0.43–0.69 (0.59)	0.24–0.68 (0.46)	0.03–0.20 (0.10)	0.17–0.66 (0.45)
	Al_2O_3	2.97–39.76 (27.64)	14.79–23.32 (19.25)	11.07–36.07 (20.45)	6.05–17.26 (11.79)	15.12–18.99 (16.77)	11.28–16.47 (14.13)	7.75–21.46 (13.79)	0.70–4.76 (2.21)	3.62–13.76 (9.09)
Palaeoclimate	CIA	78.96–95.88 (91.22)	75.62–86.23 (81.54)	80.01–98.40 (86.56)	65.1–80.58 (73.61)	50.1–75.52 (62.69)	64.37–72.33 (69.12)	70.68–84.58 (75.79)	60.87–76.02 (70.63)	62.63–72.84 (68.49)
	Cvalue	0.29–4.97 (1.91)	0.22–0.63 (0.38)	0.03–1.06 (0.37)	0.15–1.67 (0.59)	0.19–0.46 (0.31)	0.15–0.30 (0.23)	0.34–1.29 (0.79)	0.05–0.53 (0.22)	0.01–1.09 (0.24)
Palaeoproductivity	P/Ti	0.01–1.30 (0.20)	0.016–0.215 (0.12)	0.05–0.372 (0.11)	0.134–16.818 (2.03)	0.078–1.178 (0.52)	0.133–0.344 (0.24)	0.06–0.76 (0.20)	2.87–8.98 (5.19)	0.16–0.49 (0.26)
	Mo	0.75–13.11 (3.35)	0.62–5.72 (1.87)	/	2.04–189.60 (86.54)	/	0.43–3.06 (1.75)	1.50–78.50 (26.57)	6.64–33.90 (15.59)	/
Volcanic hydrothermal	Fe/Ti	1.21–77.45 (15.42)	2.04–32.86 (9.59)	1.70–37.16 (7.86)	4.95–42.39 (22.06)	9.53–34.67 (18.65)	6.45–12.61 (8.91)	8.60–17.29 (11.56)	6.83–85.38 (32.30)	6.37–14.14 (9.52)
	(Fe + Mn)/Ti	0.23–78.08 (16.02)	2.05–20.08 (9.74)	1.71–13.48 (7.99)	6.55–64.92 (25.22)	9.91–42.42 (22.05)	6.55–12.71 (9.07)	8.73–17.48 (11.69)	7.21–86.22 (32.91)	6.47–14.44 (9.65)
Redox	Ni/Co	1.62–4.82 (3.07)	1.32–3.75 (2.01)	1.94–6.85 (3.92)	1.21–2.75 (1.88)	2.19–7.66 (3.39)	1.70–2.48 (2.11)	3.60–12.01 (6.46)	2.56–4.98(3.32)	3.11–14.84 (5.92)
	δU	0.65–1.69 (1.02)	0.73–0.97 (0.84)	0.74–1.67 (0.97)	0.87–1.95 (1.76)	0.87–1.85 (1.29)	0.77–1.11 (0.88)	0.95–1.69 (1.30)	1.62–1.85 (1.75)	1.07–1.94 (1.53)
Palaeosalinity	Sr/Ba	0.29–3.71 (0.98)	0.37–0.74 (0.48)	0.03–1.98 (0.76)	0.15–1.29 (0.46)	0.18–0.51 (0.32)	0.42–1.35 (0.69)	0.54–2.53 (1.38)	0.99–57.29 (11.03)	0.24–11.82 (2.13)
Sedimentation rate	$(La/Yb)_N$	0.73–2.98 (1.83)	1.27–1.78 (1.53)	1.12–2.34 (1.65)	0.84–1.90 (1.32)	1.42–2.58 (1.97)	2.03–2.68 (2.31)	1.00–1.79 (1.37)	1.18–1.45 (1.30)	1.07–1.47 (1.28)
Stagnant environment	Mo/TOC	0.36–9.93 (1.31)	0.60–9.53 (2.45)	/	0.54–24.38 (5.62)	/	0.46–4.5 (1.92)	1.50–30.85 (10.37)	1.30–2.76 (1.78)	/
Palaeowater depth	Mn/Fe	0.002–0.018 (0.017)	0.005–0.026 (0.010)	0.003–0.058 (0.020)	0.021–0.323 (0.150)	0.027–0.459 (0.180)	0.008–0.041 (0.020)	0.004–0.032 (0.010)	0.006–0.057 (0.020)	0.008–0.023 (0.010)
	Mn/Ti	0.007–8.853 (0.631)	0.014–0.556 (0.150)	0.01–0.581 (0.140)	0.382–13.206 (3.160)	0.382–12.085 (3.400)	0.097–0.369 (0.160)	0.041–0.362 (0.120)	0.197–1.721 (0.600)	0.055–0.304 (0.140)

Notes: a) Average values in brackets; b) No data where marked with a "/"; c) The Avg. in the table indicate the average of the three formations under their corresponding sedimentary facies.

their organic-rich shale is at a high level, and the volcanic hydrothermal fluid is often associated with relative plate movement and developed at plate boundaries, which is not significantly affected by differences in sedimentary facies (Table 9, Figs. 10(c) and 10(d)). The marine shale is in the shelf facies, where the water column is the most reductive, and the bottom water is in a dysoxic-anoxic state during its deposition. In contrast, during the deposition of marine-continental transitional and continental shale, the water column is in weakly oxic-dysoxic conditions, but both are predominantly dysoxic. It is clear that the strongly reductive water column is more conducive to shale organic matter enrichment. The redox conditions (Ni/Co, δU) of the three are as follows: marine shale (average of 5.23 and 1.53) > marine-continental transitional shale (average of 3.00 and 0.94) ≈ continental shale (average of 2.46 and 1.31). Meanwhile, the paleosalinity (Sr/Ba) of the shale under the three sedimentary facies is freshwater, semi-saline, and saline respectively, showing: marine shale (average 4.85) > marine-continental transitional shale (average 0.74) > continental shale (average 0.49; Fig. 10(e) and 10(f))). From the analysis of both deposition rate and stagnation degree, it can be seen that the organic-rich shale $(La/Yb)_N$ in all three sedimentary facies lies around 1 (Fig. 10(g)), and the stagnation environment indicators (Mo/TOC) is less than 45, which indicating high deposition rate and strong stagnation and semi-stagnation characteristics (Table 9, Fig. 10(h)). These mean that the high deposition rate and strong stagnation environment can promote shale organic matter enrichment to some extent. As can be seen from Table 9 and Fig. 10(i), there is no significant correlation between palaeowater depth and the various depositional facies, which may be related to the location of deposition of the organic-rich shale.

From the above analysis, it can be seen that the differences in depositional environments of organic-rich shale under the three sedimentary facies are mainly reflected in four aspects of production factors (terrestrial clastic input and palaeoclimate) and preservation factors (palaeosalinity and redox conditions). Based on the differences between shale depositional environments, it is then possible to construct modes of organic matter enrichment during periods of shale deposition under different sedimentary phases. The continental shale was mainly developed in lake basins, where the climate was warm and humid during its deposition. The main body of bottom water was dysoxic, and the palaeosalinity was low. Previous experience showed that continental shale was strongly influenced by the continent at the lake margins and therefore has a high input of terrestrial clastic, which decreases as it extends toward the center of the lake and is moderate overall. The period of deposition was characterized by high levels of productivity and local volcanic hydrothermal fluid. By comparing the organic matter enrichment mode of the continental shale at different formations, it is clear that they are mainly influenced by palaeoproductivity, terrestrial clastic, and volcanic hydrothermal fluid, from which it can be grouped into "production mode" (Fig. 9(b)) (Zhang et al., 2017; Chen et al., 2021; Wu et al., 2021). The marine shale was mainly developed in the land shelf, and its deposition period had a warm and humid climate, while the water body was highly reductive and in a saline state. From previous analyses, it is clear that the marine shale was weakly influenced by continental influences, resulting in a low input of terrestrial clastic, while palaeoproductivity was high and possibly influenced by volcanic hydrothermal fluid in the plate junction region. The organic matter enrichment is influenced by several factors, including redox conditions and palaeosalinity, which are more controlled, while the influence of palaeoproductivity and volcanic hydrothermal fluid is relatively weak, showing a predominantly "preservation mode" (Fig. 9(c)) (Zeng et al., 2015; Chen et al., 2021; Lan and Shen, 2022; Wu et al., 2022b; Xu et al., 2022). The main depositional facies of the marine-continental transitional shale was lagoons and tidal flats, and therefore close to land, resulting in high input of terrestrial clastic and an overall hot and humid palaeoclimate for the marine-continental transitional shale. Likewise, the palaeosalinity of the marine-continental transitional shale was high and intermediate between the continental and marine shale, being semi-saline, and the water bodies were in a reduced state of dysoxic during deposition. Volcanic hydrothermal fluid was present at the plate junction at the same time as the palaeoproductivity was generally high. Organic matter enrichment is influenced by palaeoproductivity, palaeosalinity, and redox conditions, showing a "hybrid mode of preservation and production" (Fig. 9(a)) (Liu et al., 2018; Zhang et al., 2021; Wu et al., 2022b).

6 Conclusions

This study focused on the geochemical characteristics of the Upper Carboniferous Benxi Formation shale in the east-central Ordos Basin. The palaeoenvironment during their depositional period was reconstructed and the organic matter enrichment mechanism was revealed. The conclusions reached are shown below.

1) The Benxi Formation shale main elements in the study area are dominated by SiO_2, with Al_2O_3, TiO_2, and Fe_2O_3 being relatively enriched. Trace elements such as V, Cr, Co, Ni, Mo, U, and Y are enriched relative to UCC, while Zn, Zr, Sr, Ba, Ta, Hf, and Th are relatively deficient. Total rare earth elements (ΣREE) vary from 50.48 to 621.49 ppm (average 274.23 ppm), which is higher than in the NASC and UCC, and slightly higher than in the PAAS. The REE distribution pattern shows a right-sloping trend for light REEs and a flattening trend for heavy REEs.

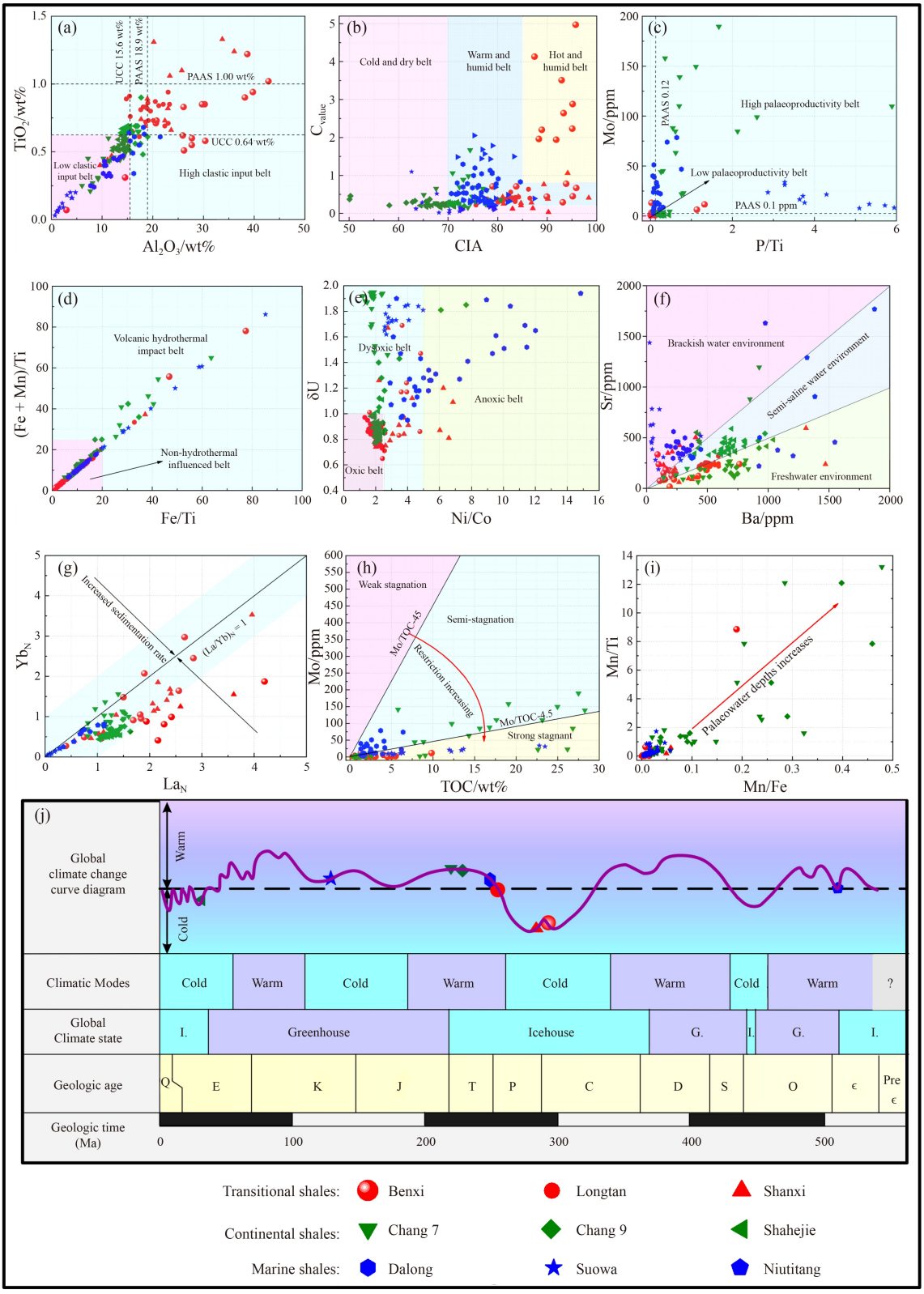

Fig. 10 Comparative map of depositional environments under differences in shale depositional facies. (a) Terrestrial clastic input; (b) palaeoclimate; (c) palaeoproductivity; (d) volcanic hydrothermal fluid; (e) redox conditions; (f) palaeosalinity; (g) sedimentation rate; (h) stagnant environment; (i) palaeowater depths; (j) global climate change curve (modified from Liang et al., 2020).

2) The tectonic setting of the Benxi Formation shale source area in the study area is mainly continental margin with a shallow palaeowater depth. It belongs to marine-continental transitional facies, where the deposition period was accompanied by strong terrestrial clastic input. The source rocks are upper crustal granite and sedimentary rocks.

3) The Benxi Formation shale was deposited in a hot and humid climate, with high palaeoproductivity and local volcanic hydrothermal fluid. At the same time, the sedimentation rate and stagnation environment of the water column were high, and the bottom water was generally in dysoxic conditions and a semi-saline sedimentary environment.

4) Multiple factors, such as palaeoproductivity, volcanic hydrothermal fluid, redox conditions, and palaeosalinity are considered to interact in influencing the enrichment and preservation of organic matter of the marine-continental transitional facies. Among these, the redox conditions have the greatest influence on organic matter preservation, while palaeosalinity and palaeoproductivity facilitate the preservation and enrichment of organic matter. The organic matter enrichment mode is a composite model combining the "preservation mode" of oxygen-poor reductive and semi-saline environment, and the "production mode" of palaeoproductivity and local volcanic hydrothermal fluid.

5) There are significant differences in the depositional environments and organic matter enrichment mechanisms of terrestrial, marine transitional, and marine organic-rich shale. The differences in depositional environments are mainly reflected in the four aspects of terrestrial detritus, palaeoclimate, redox conditions, and palaeosalinity, and the organic matter enrichment modes can be categorised as "production mode", "hybrid mode of preservation and production", and "preservation mode", respectively.

Acknowledgments This work was supported from the Natural Science Basic Research Program of Shaanxi Province (No. 2020JQ-744), China Postdoctoral Science Foundation (No. 2020M673443), Shaanxi Provincial Education Department general special project (No. 21JK0775) Opening Project of Key Laboratory of Coal Resources Exploration and Comprehensive Utilization, Ministry of Natural Resources (No. KF2021-7) and National Natural Science Foundation of China (Grant No. 4210021463).

References

Abanda P A, Hannigan R E (2006). Effect of diagenesis on trace element partitioning in shales. Chem Geol, 230(1–2): 42–59

Algeo T J, Rowe H (2012). Paleoceanographic applications of trace-metal concentration data. Chem Geol, 324–325: 6–18

Algeo T J, Tribovillard N (2009). Environmental analysis of paleoceanographic systems based on molybdenum-uranium covariation. Chem Geol, 268(3–4): 211–225

Awan R S, Liu C, Gong H, Dun C, Tong C, Chamssidini L G (2020). Paleo-sedimentary environment in relation to enrichment of organic matter of Early Cambrian black rocks of Niutitang Formation from Xiangxi area China. Mar Pet Geol, 112: 104057

Bernárdez P, Gonzalez-Alvarez R, Frances G, Prego R, Barcena M A, Romero O E (2008). Late Holocene history of the rainfall in the NW Iberian peninsula - evidence from a marine record. J Mar Syst, 72(1–4): 366–382

Chen Y, Liu S, Zhu Z, Wang Z, Sun X, Xu T (2021). Geochemical characteristics and sedimentary setting of chang 9 shale in the Upper Triassic Yanchang Formation of southeastern Ordos Basin (NW China). J Petrol Sci Eng, 196: 108081

Chen Y, Wang Y, Guo M, Wu H, Li J, Wu W, Zhao J (2020). Differential enrichment mechanism of organic matters in the marine-continental transitional shale in northeastern Ordos Basin, China: control of sedimentary environments. J Nat Gas Sci Eng, 83: 103625

Chen Y, Zhu Z, Zhang L (2019). Control actions of sedimentary environments and sedimentation rates on lacustrine oil shale distribution, an example of the oil shale in the Upper Triassic Yanchang Formation, southeastern Ordos Basin (NW China). Mar Pet Geol, 102: 508–520

Cui C, Zhang H, Liu W, Li S, Liu Y, Song H, Wu C M, Wen Z (2022). Element geochemical characteristics of shale in the first member of Benxi Formation in eastern Ordos Basin: take Zhaoxian section and M115 well in Linxian County, Shanxi as examples. Nat Gas Geosci, 33(6): 1001–1012 (in Chinese)

Cullers R L, Podkovyrov V N (2002). The source and origin of terrigenous sedimentary rocks in the Mesoproterozoic Ui group, southeastern Russia. Precambrian Res, 117(3–4): 157–183

Ding W, Zhu D, Cai J, Gong M, Chen F (2013). Analysis of the developmental characteristics and major regulating factors of fractures in marine-continental transitional shale-gas reservoirs: a case study of the Carboniferous-Permian strata in the southeastern Ordos Basin, central China. Mar Pet Geol, 45: 121–133

Ding X, Liu G, Zha M, Huang Z, Gao C, Lu X, Sun M, Chen Z, Liuzhuang X (2015). Relationship between total organic carbon content and sedimentation rate in ancient lacustrine sediments, a case study of Erlian basin, northern China. J Geochem Explor, 149: 22–29

Doner Z, Kumral M, Demirel I H, Hu Q (2019). Geochemical characteristics of the Silurian shales from the central Taurides, southern Turkey: organic matter accumulation, preservation and depositional environment modeling. Mar Pet Geol, 102: 155–175

Dong Z, Zhang J, Tang X, Liu G, Dang W, Liu Y, Tao J, Su Z (2020). Origin and diffusion of the over-mature transitional natural gas in multiple lithologic reservoirs: a case study of Carboniferous-Permian strata in the southeastern margin of Ordos Basin. Int J Coal Geol, 219: 103380

Dypvik H, Harris N B (2001). Geochemical facies analysis of fine-grained siliciclastics using Th/U, Zr/Rb and (Zr+Rb)/Sr ratios. Chem Geol, 181(1–4): 131–146

Elderfield H, Greaves M J (1982). The rare earth elements in seawater. Nature, 296(5854): 214–219

Fedo C M, Wayne Nesbitt H, Young G M (1995). Unraveling the

effects of potassium metasomatism in sedimentary rocks and paleosols, with implications for paleoweathering conditions and provenance. Geology, 23(10): 921–924

Floyd P A, Leveridge B E (1987). Tectonic environment of the Devonian Gramscatho basin, south Cornwall: framework mode and geochemical evidence from turbiditic sandstones. J Geol Soc London, 144(4): 531–542

Guo H (2020). Study on the Mechanism and Controlling Factors of Shale Gas Enrichment in Shanxi Formation-a Case Study of the Eastern Ordos Basin. Dissertation for Master Degree. Xi'an Shiyou University (in Chinese)

Haskin L A, Haskin M A, Frey F A, Wildeman T R (1968). Relative and absolute terrestrial abundances of the rare earths. In: Ahrens L H, ed. Origin Distribution of the Elements. Elsevier, 889–912

Hatch J R, Leventhal J S (1992). Relationship between inferred redox potential of the depositional environment and geochemistry of the Upper Pennsylvanian (Missourian) Stark Shale Member of the Dennis Limestone, Wabaunsee County, Kansas, U.S.A. Chem Geol, 99(1–3): 65–82

He Q, Li D, Sun Q, Wei B, Wang S (2022). Main controlling factors of marine shale compressive strength: a case study on the Cambrian Niutitang Formation in Dabashan Mountain. Energy, 260: 125100

He T, Lu S, Li W, Tan Z, Zhang X (2018). Effect of salinity on source rock formation and its control on the oil content in shales in the Hetaoyuan Formation from the Biyang Depression, Nanxiang Basin, Central China. Energy Fuels, 32(6): 6698–6707

Hoyle J, Elderfield H, Gledhill A, Greaves M (1984). The behaviour of the rare earth elements during mixing of river and sea waters. Geochim Cosmochim Acta, 48(1): 143–149

Hu T, Pang X, Jiang S, Wang Q, Xu T, Lu K, Huang C, Chen Y, Zheng X (2018). Impact of paleosalinity, dilution, redox, and paleoproductivity on organic matter enrichment in a saline lacustrine rift basin: a case study of paleogene organic-rich shale in Dongpu Depression, Bohai Bay Basin, eastern China. Energy Fuels, 32(4): 5045–5061

Hu Y, Liu Y, Guo Y, Liu W, Zhang Z, Yang X (2022). Elemental geochemical characteristics of mudstones in Upper Carboniferous Benxi Formationin southern Ordos Basin and their enlightenment to sedimentary environment. J Shandong U Sci Techn (Nat Sci), 41: 13–23

Jenkyns H C, Dickson A J, Ruhl M, Boorn S H J M (2017). Basalt-seawater interaction, the Plenus Cold Event, enhanced weathering and geochemical change: deconstructing Oceanic Anoxic Event 2 (Cenomanian-Turonian, Late Cretaceous). Sedimentology, 64(1): 16–43

Jones B, Manning D A C (1994). Comparison of geochemical indices used for the interpretation of palaeoredox conditions in ancient mudstones. Chem Geol, 111(1–4): 111–129

Khaled A, Li R, Xi S, Zhao B, Wu X, Yu Q, Zhang Y, Li D (2022). Paleoenvironmental conditions and organic matter enrichment of the Late Paleoproterozoic Cuizhuang Formation dark shale in the Yuncheng Basin, north China. J Petrol Sci Eng, 208: 109627

Lan Z, Shen J (2022). Depositional Paleo-environments of Lower Cambrian Qiongzhusi Formation in the western middle Yangtze Block and its controlling effect on the organic matter enrichment. Energies, 15(10): 3761

Latimer J C, Filippelli G M (2002). Eocene to Miocene terrigenous inputs and export production: geochemical evidence from ODP Leg 177, Site 1090. Palaeogeogr Palaeoclimatol Palaeoecol, 182(3–4): 151–164

Li D, Li R, Tan C, Zhao D, Xue T, Zhao B, Khaled A, Liu F, Xu F (2019a). Origin of silica, paleoenvironment, and organic matter enrichment in the Lower Paleozoic Niutitang and Longmaxi formations of the northwestern Upper Yangtze Plate: significance for hydrocarbon exploration. Mar Pet Geol, 103: 404–421

Li W, Li J, Lu S, Chen G, Pang X, Zhang P, He T (2022). Evaluation of gas-in-place content and gas-adsorbed ratio using carbon isotope fractionation model: a case study from Longmaxi shales in Sichuan Basin, China. Int J Coal Geol, 249: 103881

Li W, Zhang Q, Li K, Chen Q, Guo Y, Ma Y, Feng J, Zhang D (2021). Sedimentary evolution of the late Paleozoic in Ordos Basin and its adjacent areas. J Palaeogeogr, 23: 39–52 (in Chinese)

Li X, Gang W, Yao J, Gao G, Wang C, Li J, Liu Y, Guo Y, Yang S (2020). Major and trace elements as indicators for organic matter enrichment of marine carbonate rocks: a case study of Ordovician subsalt marine formations in the central-eastern Ordos Basin, north China. Mar Pet Geol, 111: 461–475

Li Y, Gao X, Meng S, Wu P, Niu X, Qiao P, Elsworth D (2019c). Diagenetic sequences of continuously deposited tight sandstones in various environments: a case study from upper Paleozoic sandstones in the Linxing area, eastern Ordos basin, China. AAPG Bull, 103(11): 2757–2783

Li Y, Wang Z, Gan Q, Niu X, Xu W (2019b). Paleoenvironmental conditions and organic matter accumulation in Upper Paleozoic organic-rich rocks in the east margin of the Ordos Basin, China. Fuel, 252: 172–187

Liang J, Tao W, Ma X (2020). Origin and paleoenvironmental reconstruction of phosphorus-bearing sandstones of the Cambrian Xinji Formation, southwestern margin of the Ordos Basin, China. Can J Earth Sci, 57(8): 903–917

Liu S, Wu C, Li T, Wang H (2018). Multiple geochemical proxies controlling the organic matter accumulation of the marine-continental transitional shale: a case study of the Upper Permian Longtan Formation, western Guizhou, China. J Nat Gas Sci Eng, 56: 152–165

Ma Y, Lu Y, Liu X, Zhai G, Wang Y, Zhang C (2019). Depositional environment and organic matter enrichment of the lower Cambrian Niutitang shale in western Hubei Province, South China. Mar Pet Geol, 109: 381–393

McLennan S M (2001). Relationships between the trace element composition of sedimentary rocks and upper continental crust. Geochem Geophys Geosyst, 2(4): n/a

Meng Q, Liu Z, Bruch A A, Liu R, Hu F (2012). Palaeoclimatic evolution during Eocene and its influence on oil shale mineralisation, Fushun basin, China. J Asian Earth Sci, 45: 95–105

Nesbitt H W, Young G M (1982). Early Proterozoic climates and plate motions inferred from major element chemistry of lutites. Nature, 299(5885): 715–717

Peters K E, Cassa M R (1994). Applied source rock geochemistry: Chapter 5: Part II. Essential Elements, 93–120

Qi H W, Hu R Z, Su W C, Qi L, Feng J Y (2004). Continental hydrothermal sedimentary siliceous rock and genesis of superlarge germanium (Ge) deposit hosted in coal: a study from the Lincang Ge deposit, Yunnan, China. Sci China Ser D Earth Sci, 47(11): 973–984

Rimmer S M (2004). Geochemical paleoredox indicators in Devonian-Mississippian black shales, central Appalachian basin (USA). Chem Geol, 206(3–4): 373–391

Rimmer S M, Thompson J A, Goodnight S A, Robl T L (2004). Multiple controls on the preservation of organic matter in Devonian-Mississippian marine black shales: geochemical and petrographic evidence. Palaeogeogr Palaeoclimatol Palaeoecol, 215(1–2): 125–154

Roser B, Korsch R J T J G (1986). Determination of tectonic setting of sandstone-mudstone suites using SiO_2 content and K_2O/Na_2O ratio. J Geol, 94(5): 635–650

Scotese C R, Song H, Mills B J W, van der Meer D G (2021). Phanerozoic paleotemperatures: the earth's changing climate during the last 540 million years. Earth Sci Rev, 215: 103503

Shi Q, Li C, Wang S, Li D, Wang S, Du F, Qiao J, Cheng Q (2022). Effect of the depositional environment on the formation of tar-rich coal: a case study in the northeastern Ordos Basin, China. J Petrol Sci Eng, 216: 110828

Song H, Wang H, Wang F, Guo R, Hu B (2016). Ichnofossils and ichnofabrics in the Lower Permian Taiyuan Formation of North China Basin. Geodin Acta, 28(1–2): 37–52

Stock C A, John J G, Rykaczewski R R, Asch R G, Cheung W W L, Dunne J P, Friedland K D, Lam V W Y, Sarmiento J L, Watson R A (2017). Reconciling fisheries catch and ocean productivity. Proc Natl Acad Sci USA, 114(8): E1441–E1449

Stüben D, Kramar U, Berner Z, Stinnesbeck W, Keller G, Adatte T (2002). Trace elements, stable isotopes, and clay mineralogy of the Elles II K-T boundary section in Tunisia: indications for sea level fluctuations and primary productivity. Palaeogeogr Palaeoclimatol Palaeoecol, 178(3–4): 321–345

Talbot M R (1988). The origins of lacustrine oil source rocks: evidence from the lakes of tropical Africa. Geological Society. 40(6): 29–43

Tang D, Shi X, Zhao X, Wang X, Song G (2015). Mo-U Covariation as an important proxy for sedimentary environment redox conditions progress, problems and prospects. Geoscience, 29(1): 1 (in Chinese)

Tang X, Zhang J, Wang X, Yu B, Ding W, Xiong J, Yang Y, Wang L, Yang C (2014). Shale characteristics in the southeastern Ordos Basin, China: implications for hydrocarbon accumulation conditions and the potential of continental shales. Int J Coal Geol, 128–129: 32–46

Taylor S R, McLennan S M (1985). The Continental Crust: Its Composition and Evolution. Blackwell Scientific Pub

Taylor S R, McLennan S M (1995). The geochemical evolution of the continental crust. Rev Geophys, 33(2): 241–265

Tenger, Liu W, Xu Y, Chen J (2006). Comprehensive geochemical identification of highly evolved marine carbonate rocks as hydrocarbon-source rocks as exemplified by the Ordos Basin. Sci China Ser D Earth Sci, 49(4): 384–396

Tribovillard N, Algeo T J, Lyons T, Riboulleau A (2006). Trace metals as paleoredox and paleoproductivity proxies: an update. Chem Geol, 232(1–2): 12–32

Tyson R V (2001). Sedimentation rate, dilution, preservation and total organic carbon: some results of a modelling study. Org Geochem, 32(2): 333–339

Wang Q, Jiang F, Ji H, Jiang S, Liu X, Zhao Z, Wu Y, Xiong H, Li Y, Wang Z (2020). Effects of paleosedimentary environment on organic matter enrichment in a saline lacustrine rift basin - A case study of Paleogene source rock in the Dongpu Depression, Bohai Bay Basin. J Petrol Sci Eng, 195: 107658

Wedepohl K J P, Earth C (1971). Environmental influences on the chemical composition of shales and clays. Phys Chem Earth, 8: 307–333

Wei Z, Wang Y, Wang G, Zhang T, He W, Ma X, Yu X (2020). Enrichment mechanism of the Upper Carboniferous-Lower Permian transitional shale in the east margin of the Ordos Basin, China: evidence from geochemical proxies. Geofluids, 2020: 1–14

Wignall P B, Twitchett R J (1996). Oceanic anoxia and the end Permian mass extinction. Science, 272(5265): 1155–1158

Wu J, Zhang Y, Zhou H (2020). Groundwater chemistry and groundwater quality index incorporating health risk weighting in Dingbian County, Ordos basin of northwest China. Chem Erde, 80(4): 125607

Wu Y, Liu C, Liu Y, Gong H, Awan R S, Li G, Zang Q (2022a). Geochemical characteristics and the organic matter enrichment of the Upper Ordovician Tanjianshan Group, Qaidam Basin, China. J Petrol Sci Eng, 208: 109383

Wu Z, He S, He Z, Li X, Zhai G, Huang Z (2022b). Petrographical and geochemical characterization of the Upper Permian Longtan formation and Dalong Formation in the Lower Yangtze region, South China: implications for provenance, paleoclimate, paleoenvironment and organic matter accumulation mechanisms. Mar Pet Geol, 139: 105580

Wu Z, Zhao X, Li J, Pu X, Tao X, Shi Z, Sun Y (2021). Paleoenvironmental modes and organic matter enrichment mechanisms of lacustrine shale in the Paleogene Shahejie Formation, Qikou Sag, Bohai Bay Basin. Energy Rep, 7: 9046–9068

Xu L, Huang S, Liu Z, Zhang Y, Wen Y, Zhou X, Chen W, Ren Z, Wen J (2022). Paleoenvironment evolutionary characteristics of Niutitang shale in Western Hubei, Middle Yangtze, China. ACS Omega, 7(28): 24365–24383

Xu L, Lehmann B, Zhang X, Zheng W, Meng Q (2014). Trace element distribution in black shales from the Kunyang phosphorite deposit and its geological significances. Acta Petrol Sin, 30: 1817–1827

Yamamoto K (1987). Geochemical characteristics and depositional environments of cherts and associated rocks in the Franciscan and Shimanto Terranes. Sediment Geol, 52(1–2): 65–108

Yang K, Zhang B, Yao Y, Yang H, Zhang H, Xiao W, Wang Y (2022). Organic matter accumulation mechanism and characteristics in marine-continental transitional shale: a case study of the upper Permian Longtan Formation from the Well F5 in Sichuan Basin,

China. J Petrol Sci Eng, 208: 109604

Yang R, Ma T, Liu W, Fang Y, Xing L (2019). Coupled hydro-mechanical analysis of gas production in fractured shale reservoir by random fracture network modeling. Int J Appl Mech, 11(3): 1950031

Yang X, Yan D, Zhang B, Zhang L, Wei X, Li T, He J, Shangguan Y, Zhang M, She X (2020). The depositional mechanism of organic-rich siliceous shales in Upper Yangtze area: response to the Kwangsian Orogeny in south China. J Petrol Sci Eng, 192: 107310

Yang Y T, Li W, Ma L (2005). Tectonic and stratigraphic controls of hydrocarbon systems in the Ordos Basin: a multicycle cratonic basin in central China. AAPG Bull, 89(2): 255–269

Yu W, Tian J, Wang F, Liang Q, Yang T, Kneller B, Liang X (2022). Sedimentary environment and organic matter enrichment of black mudstones from the upper Triassic Chang-7 member in the Ordos Basin, northern China. J Asian Earth Sci, 224: 105009

Zeng S, Wang J, Fu X, Chen W, Feng X, Wang D, Song C, Wang Z (2015). Geochemical characteristics, redox conditions, and organic matter accumulation of marine oil shale from the Changliang Mountain area, northern Tibet, China. Mar Pet Geol, 64: 203–221

Zhang K, Li Z, Jiang S, Jiang Z, Wen M, Jia C, Song Y, Liu W, Huang Y, Xie X, Liu T, Wang P, Shan C, Wu Y (2018a). Comparative analysis of the siliceous source and organic matter enrichment mechanism of the Upper Ordovician-Lower Silurian Shale in the Upper-Lower Yangtze Area. Minerals (Basel), 8(7): 283

Zhang L, Kou Z, Wang H, Zhao Y, Dejam M, Guo J, Du J (2018b). Performance analysis for a model of a multi-wing hydraulically fractured vertical well in a coalbed methane gas reservoir. J Petrol Sci Eng, 166: 104–120

Zhang L, Zhao Q, Peng S, Qiu Z, Feng C, Zhang Q, Wang Y, Dong D, Zhou S (2021). Paleoenvironment and organic matter accumulation mechanism of marine-continental transitional shales: outcrop characterizations of the Carboniferous-Permian strata, Ordos Basin, north China. Energies, 14(21): 7445

Zhang P, Yang M, Lu J, Shao L, Wang Z, Hilton J (2022). Low-latitude climate change linked to high-latitude glaciation during the late paleozoic ice age: evidence from terrigenous detrital kaolinite. Front Earth Sci (Lausanne), 10: 956861

Zhang W, Yang H, YangY, Kong Q, Wu K (2008). Petrology and element geochemistry and development environment of Yanchang Formation Chang-7 high quality source rocks in Ordos Basin. Geochimica, 37(1): 59–64

Zhang W, Yang W, Xie L (2017). Controls on organic matter accumulation in the Triassic Chang 7 lacustrine shale of the Ordos Basin, central China. Int J Coal Geol, 183: 38–51

Zhao B, Li R, Qin X, Wang N, Zhou W, Khaled A, Zhao D, Zhang Y, Wu X, Liu Q (2021). Geochemical characteristics and mechanism of organic matter accumulation of marine-continental transitional shale of the lower permian Shanxi Formation, southeastern Ordos Basin, north China. J Petrol Sci Eng, 205: 108815

Zhou T, Zhou Y, Zhao H, Li M, Mu H (2022). Depositional setting and enrichment mechanism of organic matter of Lower Cretaceous shale in Ri-Qing-Wei Basin in the Central Sulu Orogenic Belt. Front Earth Sci (Lausanne), 9: 808916